Finite-displacement computation of the electron-phonon interaction within the projector augmented-wave method

L. Chaput,[1,*] Atsushi Togo,[2,†] and Isao Tanaka[2,3,4,‡]

[1]*Université de Lorraine, LEMTA, Centre National de la Recherche Scientifique, Unité Mixte de Recherche 7563, BP 70239, 54506 Vandœuvre Cedex, France*

[2]*Center for Elements Strategy Initiative for Structural Materials, Kyoto University, Sakyo, Kyoto 606-8501, Japan*

[3]*Department of Materials Science and Engineering, Kyoto University, Sakyo, Kyoto 606-8501, Japan*

[4]*Nanostructures Research Laboratory, Japan Fine Ceramics Center, Atsuta, Nagoya 456-8587, Japan*

(Received 30 August 2019; published 27 November 2019)

A computational method has been developed to compute the electron-phonon interactions using the projector augmented wave method and finite displacements. Aluminium and diamond crystals are considered to test our strategy. It is found that the potential derivatives are quickly convergent with respect to the supercell size. Moreover the method is found to be efficient enough to densely sample the Brillouin zone and compute the Eliashberg function and phonon lifetime without requiring the use to interpolations.

DOI: 10.1103/PhysRevB.100.174304

I. INTRODUCTION

In material science, high throughput, and the subsequent data mining and machine learning algorithms, have become popular techniques to understand physical properties, or correlation between physical properties, and to guide the discovery of novel materials [1–4]. In many cases, the success of theses approaches is inherited from the quality of the underlying density functional theory (DFT) calculations, which provides most of the microscopic information needed to compute measurable properties, and allows systematic applicability to a variety of materials.

In bulk crystals, the electron-phonon interaction is the basic mechanism that allows the electron and ion systems to exchange energy. Therefore the strength of this interaction may controls or affects the value of very different physical properties such as the critical temperature of superconductors [5,6], the electric and thermal conductivity of metals [7], thermal melting under irradiation [8], or ferroelectric instabilities [9].

If those properties are to be investigated using high throughput calculations, an accurate, efficient, and automatic method is necessary for the computation of the electron-phonon interaction. Electron-phonon interactions can be accurately computed using density functional perturbation theory (DFPT) [10], or its extension to the *GW* method [11], but the evaluation of most of the above mentioned quantities require a very dense sampling of reciprocal space which makes this approach computationally expensive. It has been shown that it is possible to linearly interpolate the DFTP results to a finer grid to obtain a convergent evaluation of several physical properties [12], but nowadays most of the *ab initio* calculation of the electron-phonon interaction are performed after a Wannier transformation of the Bloch states followed by a back Fourier interpolation to reciprocal space [13]. This approach has many advantages. At first it is physically transparent, formally simple, and quite efficient. However the Wannier transformation itself may be difficult [14–16], leading to a computation which is not fully automatic or computer controlled, and consequently making the high throughput computing more difficult. Therefore an alternative to the computation of the electron-phonon interaction based on Wannier-Fourier interpolation may be useful in some cases.

In this paper, based on our previous works on phonon and phonon-phonon interactions [17–20], we propose to compute the electron-phonon interaction from the finite displacement method and implemented our strategy when the projector augmented wave (PAW) method is used to solve the independent particle Schrödinger equation of DFT. Our approach require no interpolation of the electron-phonon coupling function since the evaluation of the matrix elements is performed in real space using efficient grid techniques. Also, this strategy requires no additional computer implementations when using different exchange correlation potentials.

The paper is organized as follow. In Sec. II, for further reference, the electron-phonon interaction is derived from the reduced dynamics of the ions in the field of the electrons. In particular, it is shown that the electrons influence the ions dynamics through a vector potential much in the same way an electromagnetic field influences the electrons motion. In Sec. III, the electron-phonon interaction is expressed using the quantities defining in the PAW method. In Sec. IV, we provide the details of the numerical implementation. Finally, in Sec. V, several quantities are computed for the diamond and aluminium test cases to evidence the good accuracy and efficiency of our method. The paper is concluded in Sec. VI.

*laurent.chaput@univ-lorraine.fr
†togo.atsushi@gmail.com
‡tanaka@cms.mtl.kyoto-u.ac.jp

II. THE INTERACTION OF PHONONS WITH ELECTRONS

A. The nuclear Hamiltonian

The Schrödinger equation for the electronic and nuclear degrees of freedom is written as

$$i\hbar\frac{\partial}{\partial t}\Psi(\mathbf{r},\mathbf{R},t)=H\Psi(\mathbf{r},\mathbf{R},t), \tag{1}$$

where $\mathbf{r}$ and $\mathbf{R}$ denotes the set of electronic and atomic vector positions, $\mathbf{r}=\{\mathbf{r}_i, i=1,\ldots,N_e\}$ and $\mathbf{R}=\{\mathbf{R}_{l\tau}\}$. The index l is used to label the N primitive unit cells of the crystal and τ the N_a atoms in those unit cells. N_e is the number of electrons.

The Hamiltonian can be split into the kinetic energy of the nucleus plus an electronic part, which is independent of the nuclear momentums,

$$H=T_n+H_e, \tag{2}$$

$$T_n=\sum_{l\tau\alpha}-\frac{\hbar^2}{2M_\tau}\frac{\partial^2}{\partial R^2_{l\tau\alpha}}, \tag{3}$$

$$H_e=\sum_{i\alpha}-\frac{\hbar^2}{2m}\frac{\partial^2}{\partial r^2_{i\alpha}}+\frac{1}{2}\sum_{i\neq j}\frac{e^2}{4\pi\epsilon_0|\mathbf{r}_i-\mathbf{r}_j|} \tag{4}$$

$$+\sum_{il\tau}\frac{-e^2Z_\tau}{4\pi\epsilon_0|\mathbf{r}_i-\mathbf{R}_{l\tau}|}+\frac{1}{2}\sum_{l\tau\neq l'\tau'}\frac{e^2Z_\tau Z_{\tau'}}{4\pi\epsilon_0|\mathbf{R}_{l\tau}-\mathbf{R}_{l'\tau'}|}. \tag{5}$$

In the above equations, α label the Cartesian components, M_τ and Z_τ are the atomic masses and atomic numbers, and e and ϵ_0 are the fundamental constants for the electronic charge and vacuum permittivity.

The eigenstates and eigenenergies of the electronic Hamiltonian are parametrized by the nuclear positions,

$$H_e\Phi_i(\mathbf{r};\mathbf{R})=E_i(\mathbf{R})\Phi_i(\mathbf{r};\mathbf{R}), \tag{6}$$

and, according to Born and Huang [21], the total wave function can be expanded with respect to those electronic eigenstates,

$$\Psi(\mathbf{r},\mathbf{R},t)=\sum_i\chi_i(\mathbf{R},t)\Phi_i(\mathbf{r};\mathbf{R}). \tag{7}$$

The coefficients of this expansion, squared, gives the probability density at time t for the nuclei to be in configuration $\mathbf{R}$ and the electronic system in state i. Substituting Eq. (7) into Eq. (1), multiplying with $\Phi_i(\mathbf{r};\mathbf{R})^*$ and integrating over the electronic degrees of freedom, one obtains an equation for the $\chi_i(\mathbf{R},t)$. Defining the multicomponent phonon wave function,

$$\chi(\mathbf{R},t)=[\chi_1(\mathbf{R},t)\ \chi_2(\mathbf{R},t)\ \cdots]^t, \tag{8}$$

this equation can be written as

$$i\hbar\frac{\partial}{\partial t}\chi(\mathbf{R},t)=H_n\chi(\mathbf{R},t) \tag{9}$$

$$=(H_{\mathrm{BO}}+H_{\mathrm{CBO}})\chi(\mathbf{R},t), \tag{10}$$

where the matrix operators H_{BO} and H_{CBO} are defined by

$$[H_{\mathrm{BO}}]_{ij}=(T_n+E_i(\mathbf{R}))\delta_{ij}, \tag{11}$$

$$[H_{\mathrm{CBO}}]_{ij}=2\sum_{l\tau}-\frac{\hbar^2}{2M_\tau}\langle\Phi_i|\frac{\partial}{\partial\mathbf{R}_{l\tau}}|\Phi_j\rangle\cdot\frac{\partial}{\partial\mathbf{R}_{l\tau}}+\langle\Phi_i|T_n|\Phi_j\rangle, \tag{12}$$

where H_{BO} is the Born-Oppenheimer Hamiltonian and H_{CBO} a correction. The splitting of the nuclear Hamiltonian H_n into an operator which is diagonal in the basis of electronic eigenstates (H_{BO}) and a non diagonal part (H_{CBO}) is the conventional way of writing the Schrödinger equation for $\chi(\mathbf{R},t)$. Indeed, the neglect of H_{CBO} leads to the Born-Oppenheimer approximation where the equations for the different electronic states decouples [21].

However, a most illuminating form can also be obtained if H_n is expressed in term of the electronic matrix elements of the nuclear momentum operators,

$$\mathbf{A}^{ij}_{l\tau}=\langle\Phi_i|-i\hbar\frac{\partial}{\partial\mathbf{R}_{l\tau}}|\Phi_j\rangle. \tag{13}$$

Then, noticing that

$$-\hbar^2\langle\Phi_i|\sum_\alpha\frac{\partial^2}{\partial R^2_{l\tau\alpha}}|\Phi_j\rangle=\left(-i\hbar\frac{\partial}{\partial\mathbf{R}_{l\tau}}\right)\cdot\mathbf{A}^{ij}_{l\tau}+\sum_k\mathbf{A}^{ik}_{l\tau}\cdot\mathbf{A}^{kj}_{l\tau}, \tag{14}$$

we obtain

$$H_n=\sum_{l\tau}\frac{1}{2M_\tau}(\mathbf{P}_{l\tau}+\mathbf{A}_{l\tau})^2+\mathbf{V}, \tag{15}$$

where we have defined the matrices

$$[\mathbf{P}_{l\tau}]_{ij}=\delta_{ij}\left(-i\hbar\frac{\partial}{\partial\mathbf{R}_{l\tau}}\right), \tag{16}$$

$$[\mathbf{A}_{l\tau}]_{ij}=\mathbf{A}^{ij}_{l\tau}=\langle\Phi_i|-i\hbar\frac{\partial}{\partial\mathbf{R}_{l\tau}}|\Phi_j\rangle, \tag{17}$$

$$[\mathbf{V}]_{ij}=\delta_{ij}E_i(\mathbf{R}). \tag{18}$$

Clearly the matrix $\mathbf{A}_{l\tau}$ is formally acting on the multicomponents phonon wave function as the electromagnetic vector potential is acting on an electronic wave function. This matrix alone determine the coupling of the nuclear and electronic degrees of freedom.

B. The phonon-electron Hamiltonian

In the previous section, we have evidenced that the matrix of first-order derivatives determines the coupling between the electronic and nuclear degrees of freedom. Therefore it can be used to express the interaction of the phonons with electrons.

Phonons are defined in the harmonic approximation, when in the Born-Oppenheinmer Hamiltonian, Eq. (11), the atomic motion is simplified by expanding the potential energy around a reference (equilibrium) configuration $\{\mathbf{R}^0_{l\tau}\}$, and truncating this expansion to second order to obtain a function which is quadratic in the ions positions. Phonons are then the single-particle excitations of this approximate Hamiltonian. Since different choices of phases for the phonon eigenvectors are possible, we review this approximation in Appendix A. In particular, it is shown that with our conventions the nuclear

derivative operator can be written in terms of the phonon creation and annihilation operators as

$$-i\hbar\frac{\partial}{\partial \mathbf{R}_{l\tau}} = -i\sqrt{M_\tau}\sum_{\mathbf{q}j}\sqrt{\frac{\hbar\omega_{\mathbf{q}j}}{2}}\frac{e^{i\mathbf{q}\cdot\mathbf{l}}\mathbf{e}_\tau^{\mathbf{q}j}}{\sqrt{N}}(a_{\mathbf{q}j}-a^+_{-\mathbf{q}j}). \quad (19)$$

The second-order term in Eq. (12) is a scalar which has no matrix elements between states with a different number of phonons. Therefore it will not be discussed in the following since we will focus on phonon scattering. This leads us to define the phonon-electron interaction as

$$[H_{pe}]_{ij} = \sum_{l\tau}\frac{1}{M_\tau}\mathbf{A}^{ij}_{l\tau}\cdot\left(-i\hbar\frac{\partial}{\partial \mathbf{R}_{l\tau}}\right). \quad (20)$$

It can be written as

$$[H_{pe}]_{ij} = \frac{1}{\sqrt{N}}\sum_{\mathbf{q}j}\sum_{l\tau}(-i\omega_{\mathbf{q}j})\mathbf{A}^{ij}_{l\tau}\cdot\delta\mathbf{R}^{\mathbf{q}j}_{l\tau}(a_{\mathbf{q}j}-a^+_{-\mathbf{q}j}), \quad (21)$$

where we have defined the atomic displacement in mode $\mathbf{q}j$ as

$$\delta\mathbf{R}^{\mathbf{q}j}_{l\tau} = \sqrt{\frac{\hbar}{2M_\tau\omega_{\mathbf{q}j}}}\mathbf{e}^{\mathbf{q}j}_\tau e^{i\mathbf{q}\cdot\mathbf{R}_l}. \quad (22)$$

If a single-particle approximation is used, such that the Kohn-Sham ansatz in density functional theory (DFT), the Φ_i are Slater determinants. In a crystal, such Slater determinants are defined by the list of occupation number over the first Brillouin zone, $\{f_{\mathbf{k}n}\}$, where $\mathbf{k}$ and n are the electron wave vectors and band indexes. Therefore we have

$$\Phi_i(\mathbf{r}) = \langle\mathbf{r}|\{f_{\mathbf{k}n}\}\rangle \quad (23)$$

$$= \frac{1}{\sqrt{N_e!}}\det|\varphi_{\mathbf{k}_1n_1}(\mathbf{r})\varphi_{\mathbf{k}_2n_2}(\mathbf{r})\ldots\varphi_{\mathbf{k}_{N_e}n_{N_e}}(\mathbf{r})|, \quad (24)$$

where $\det(\cdot)$ is the determinant of the single-particle Bloch states $\varphi_{\mathbf{k}n}$ with energy $\epsilon_{\mathbf{k}n}$, and the $\mathbf{k}_in_i$ are the occupied states.

In this single-particle approximation, the derivative couplings $\mathbf{A}^{ij}_{l\tau}$ can be expressed in term of the $\varphi_{\mathbf{k}n}$. Indeed the nuclear derivative acts as a one particle operator on a Slater determinant,

$$\frac{\partial}{\partial \mathbf{R}_{l\tau}}\det|\varphi_{\mathbf{k}_1n_1}(\mathbf{r})\varphi_{\mathbf{k}_2n_2}(\mathbf{r})\ldots\varphi_{\mathbf{k}_{\mathbf{N_e}}n_{N_e}}(\mathbf{r})|$$

$$= \sum_{i=1}^{N_e}\begin{vmatrix} \varphi_{\mathbf{k}_1n_1}(\mathbf{r}_1) & \cdots & \frac{\partial\varphi_{\mathbf{k}_1n_1}(\mathbf{r}_i)}{\partial\mathbf{R}_{l\tau}} & \cdots & \varphi_{\mathbf{k}_1n_1}(\mathbf{r}_{N_e}) \\ \varphi_{\mathbf{k}_2n_2}(\mathbf{r}_1) & \cdots & \frac{\partial\varphi_{\mathbf{k}_2n_2}(\mathbf{r}_i)}{\partial\mathbf{R}_{l\tau}} & \cdots & \varphi_{\mathbf{k}_2n_2}(\mathbf{r}_{N_e}) \\ \vdots & & \vdots & & \vdots \\ \varphi_{\mathbf{k}_{N_e}n_{N_e}}(\mathbf{r}_1) & \cdots & \frac{\partial\varphi_{\mathbf{k}_{N_e}n_{N_e}}(\mathbf{r}_i)}{\partial\mathbf{R}_{l\tau}} & \cdots & \varphi_{\mathbf{k}_{N_e}n_{N_e}}(\mathbf{r}_{N_e}) \end{vmatrix}, \quad (25)$$

therefore we obtain

$$\mathbf{A}^{ij}_{l\tau} = \sum_{\mathbf{k}n}\sum_{\mathbf{k}'n'}\gamma^{ij}_{\mathbf{k}n,\mathbf{k}'n'}\langle\varphi_{\mathbf{k}n}|-i\hbar\frac{\partial}{\partial\mathbf{R}_{l\tau}}|\varphi_{\mathbf{k}'n'}\rangle \quad (26)$$

$$= \sum_{\mathbf{k}n}\sum_{\mathbf{k}'n'}\gamma^{ij}_{\mathbf{k}n,\mathbf{k}'n'}\mathbf{A}^{l\tau}_{\mathbf{k}n,\mathbf{k}'n'}, \quad (27)$$

where $\gamma^{ij}_{\mathbf{k}n,\mathbf{k}'n'} = \langle\Phi_i|c^+_{\mathbf{k}n}c_{\mathbf{k}'n'}|\Phi_j\rangle$ is the one-particle transition density matrix, and $c^+_{\mathbf{k}n}$ and $c_{\mathbf{k}'n'}$ are the electron creation and annihilation operators in the Bloch states $\varphi_{\mathbf{k}n}$ and $\varphi_{\mathbf{k}'n'}$. Clearly, the diagonal elements of the matrix $\mathbf{A}^{l\tau}_{\mathbf{k}n,\mathbf{k}'n'}$ are simply Berry connections [22].

Using Eq. (27) in the above equation for H_{pe}, we obtain

$$[H_{pe}]_{ij} = \frac{1}{\sqrt{N}}\sum_{\mathbf{q}j}\sum_{\mathbf{k}n}\sum_{\mathbf{k}'n'}\left(\sum_{l\tau}(-i\omega_{\mathbf{q}j})\mathbf{A}^{l\tau}_{\mathbf{k}n,\mathbf{k}'n'}\cdot\delta\mathbf{R}^{\mathbf{q}j}_{l\tau}\right) \times\gamma^{ij}_{\mathbf{k}n,\mathbf{k}'n'}(a_{\mathbf{q}j}-a^+_{-\mathbf{q}j}) \quad (28)$$

or, if the lattice periodicity is used,

$$[H_{pe}]_{ij} = \frac{1}{\sqrt{N}}\sum_{\mathbf{q}j}\sum_{\mathbf{k}n}\sum_{\mathbf{k}'n'}\left(\sum_{\tau}(-i\omega_{\mathbf{q}j})\mathbf{A}^{0\tau}_{\mathbf{k}n,\mathbf{k}'n'}\cdot\delta\mathbf{R}^{\mathbf{q}j}_{0\tau}\right) \times\Delta(\mathbf{q}+\mathbf{k}'-\mathbf{k})\gamma^{ij}_{\mathbf{k}n,\mathbf{k}'n'}(a_{\mathbf{q}j}-a^+_{-\mathbf{q}j}), \quad (29)$$

where the function $\Delta(\mathbf{q})$ is 1 when $\mathbf{q}$ is a reciprocal lattice vector, and 0 otherwise. To obtain the above equation, we have used electronic wave functions normalized to 1 over a primitive unit cell to compute $\mathbf{A}^{0\tau}_{\mathbf{k}n,\mathbf{k}'n'}$ in Eq. (29); this evidences the $1/\sqrt{N}$ scaling of the Hamiltonian.

Finally the interaction Hamiltonian of phonons with electrons is written as

$$H_{pe} = \frac{1}{\sqrt{N}}\sum_{\mathbf{q}j}\sum_{\mathbf{k}n}\sum_{\mathbf{k}'n'}g^p(\mathbf{k}n,\mathbf{k}'n',\mathbf{q}j)(a_{\mathbf{q}j}-a^+_{-\mathbf{q}j})c^+_{\mathbf{k}n}c_{\mathbf{k}'n'}, \quad (30)$$

where the coupling function is defined by

$$g^p(\mathbf{k}n,\mathbf{k}'n',\mathbf{q}j) = -i\omega_{\mathbf{q}j}\sum_\tau\left(\mathbf{A}^{0\tau}_{\mathbf{k}n,\mathbf{k}'n'}\cdot\delta\mathbf{R}^{\mathbf{q}j}_{0\tau}\right)\Delta(\mathbf{q}+\mathbf{k}'-\mathbf{k}). \quad (31)$$

From the point of view of electrons, the above equation shows that the single-particle excitation of an electron from a state $\varphi_{\mathbf{k}'n'}$ to $\varphi_{\mathbf{k}n}$ can only happen using a phonon of wave vector $\mathbf{q}$ which allows conservation of the crystal momentum. From the point of view of phonons, the above equation shows that every phonon mode will be subject to a potential, resulting from the electronic pair excitations, leading to the creation and annihilation of phonons in that mode. This form is therefore appropriate for many body perturbation theory in the phonon system, and transport computations. For example, it gives immediately the Boltzmann decay rate for phonons [23]

$$\frac{1}{\tau_{\mathbf{q}j}} = 2\frac{2\pi}{\hbar}\frac{1}{N}\sum_{\mathbf{k}n}\sum_{\mathbf{k}'n'}\Delta(\mathbf{q}+\mathbf{k}'-\mathbf{k})(f_{\mathbf{k}'n'}-f_{\mathbf{k}n}) \times|g^p(\mathbf{k}n,\mathbf{k}'n',\mathbf{q}j)|^2\delta(\epsilon_{\mathbf{k}n}-\epsilon_{\mathbf{k}'n'}-\hbar\omega_{\mathbf{q}j}). \quad (32)$$

It should be noted that the coupling function we have defined above is not exactly the one used to study the many body electronic problem subject to a perturbation from the lattice [24]. They are however closely related since

$$g^e(\mathbf{k}n,\mathbf{k}'n',\mathbf{q}j) = \frac{\epsilon_{\mathbf{k}n}-\epsilon_{\mathbf{k}'n'}}{\hbar\omega_{\mathbf{q}j}}g^p(\mathbf{k}n,\mathbf{k}'n',\mathbf{q}j). \quad (33)$$

In particular, they become equal for processes conserving energy.

In the usual approach, based on Bloch [25] and Fröhlich [26] works, we look at the problem from the electrons point of view. The lattice vibrations create a change in the potential seen by electrons, which is then considered as a perturbation which scatter the electrons between states of the unperturbed system. g^e is the probability amplitude for such a transition. In the present approach the interaction of the phonons with electrons is considered from the phonons point of view, as a correction to the Born-Oppenheimer Hamiltonian, which itself rely on the use of the adiabatic electronic wave functions. In this approximation, the electronic energy, which plays the role of potential energy for the ions, is computed at the instantaneous positions of the ions. However the effect on the ions of the change in the electronic wave functions in the course of the motion is neglected. It is that correction, Eq. (12), that we use to define the interaction of the phonon with the electrons. Equation (33) shows that for energy conserving processes both point of views are equivalent because the transition probabilities are the same. The reason for that equivalence can be understood considering that the change in the wave function, considered in the present approach, can be related to the change in the potential used in the Bloch and Fröhlich approach, for example, using perturbation theory. For higher-order processes, both approaches remains equivalent as long as expectation values are consistently computed to the same order [27,28]. We postpone this question to a future study, and now focus on the computation of $\mathbf{A}^{0\tau}_{\mathbf{k}n,\mathbf{k}'n'}$.

III. THE PROJECTOR AUGMENTED-WAVE METHOD

A. Formalism

In the next section, we will derive an explicit formula for the computation of $\mathbf{A}^{0\tau}_{\mathbf{k}n,\mathbf{k}'n'} = \mathbf{A}^{\tau}_{\mathbf{k}n,\mathbf{k}'n'}$ within the projector augmented-wave (PAW) formalism. Therefore, in this section, we briefly review the main equations of the PAW method. For a more comprehensive presentation of the method, the readers should refer to the original references [29,30].

In a single-particle approach such that the DFT with the Kohn-Sham ansatz, the eigenstates Φ_i are Slater determinants built from Bloch wave functions obtained from a single-particle Schrödinger equation,

$$h\varphi_{\mathbf{k}n} = \Big(-\frac{\hbar^2}{2m}\nabla^2 + v(\mathbf{r})\Big)\varphi_{\mathbf{k}n} = \epsilon_{\mathbf{k}n}\varphi_{\mathbf{k}n}, \tag{34}$$

where $v(\mathbf{r})$ is a local potential.

When the PAW method is used to solve that equation, the Bloch wave functions are written as

$$\varphi_{\mathbf{k}n}(\mathbf{r}) = \tilde{\varphi}_{\mathbf{k}n}(\mathbf{r}) + \sum_{l\tau L}[\phi_{l\tau L}(\mathbf{r}) - \tilde{\phi}_{l\tau L}(\mathbf{r})]\langle\tilde{p}_{l\tau L}|\tilde{\varphi}_{\mathbf{k}n}\rangle, \tag{35}$$

where

$$\begin{aligned}\tilde{\varphi}_{\mathbf{k}n}(\mathbf{r}) &= \sum_{\mathbf{G}} a_{\mathbf{k}n}(\mathbf{G})\frac{e^{i(\mathbf{k}+\mathbf{G})\cdot\mathbf{r}}}{\sqrt{\Omega}} \\ &= \sum_{\mathbf{G}} a_{\mathbf{k}n}(\mathbf{G})\langle\mathbf{r}|\mathbf{k}+\mathbf{G}\rangle\end{aligned} \tag{36}$$

is a pseudo-wave-function which is supposed to have a rapidly convergent plane wave expansion. $\phi_{l\tau L}$ and $\tilde{\phi}_{l\tau L}$ are atomic and pseudoatomic orbitals, centered at positions $\mathbf{R}_{l\tau}$, and with principal, orbital and azimuthal quantum numbers summarized in the mixed index $L = (n, l, m)$. For example,

$$\phi_{l\tau L}(\mathbf{r}) = \phi_{nlm}(\mathbf{r}; l\tau) = \phi_{nlm}(\mathbf{r} - \mathbf{R}_{l\tau}), \tag{37}$$

$$\phi_{nlm}(\mathbf{r}) = R_{nl}(r)S_{lm}(\hat{r}). \tag{38}$$

$S_{lm}(\hat{r})$ are real spherical harmonics at $\hat{r} = \mathbf{r}/r$. R_{nl} are radial functions defined within the sphere $\mathcal{S}_{l\tau}$ centered at $\mathbf{R}_{l\tau}$ and with radius $s_{l\tau}$.

The functions $\tilde{p}_{l\tau L}$ appearing in Eq. (35) are known as projectors. They are the dual functions of $\tilde{\phi}_{l\tau L}$ in $\mathcal{S}_{l\tau}$ which go to zero at $s_{l\tau}$. Therefore we have

$$\langle\tilde{p}_{l\tau L}|\tilde{\phi}_{l\tau L'}\rangle = \delta_{LL'}, \tag{39}$$

and it is assumed that this set of functions is complete in $\mathcal{S}_{l\tau}$,

$$1 = \sum_{L}|\tilde{\phi}_{l\tau L}\rangle\langle\tilde{p}_{l\tau L}|. \tag{40}$$

Substituting the above definitions into Eq. (35), one obtains

$$\begin{aligned}\varphi_{\mathbf{k}n}(\mathbf{r}) &= \sum_{\mathbf{G}} a_{\mathbf{k}n}(\mathbf{G})\langle\mathbf{r}|\mathcal{T}|\mathbf{k}+\mathbf{G}\rangle \\ &= \sum_{\mathbf{G}} a_{\mathbf{k}n}(\mathbf{G})\chi_{\mathbf{k}+\mathbf{G}}(\mathbf{r})\end{aligned} \tag{41}$$

with

$$\mathcal{T} = 1 + \sum_{l\tau L}[|\phi_{l\tau L}\rangle - |\tilde{\phi}_{l\tau L}\rangle]\langle\tilde{p}_{l\tau L}|, \tag{42}$$

$$\chi_{\mathbf{k}+\mathbf{G}}(\mathbf{r}) = \langle\mathbf{r}|\mathcal{T}|\mathbf{k}+\mathbf{G}\rangle. \tag{43}$$

The previous equation can also be written as

$$|\varphi_{\mathbf{k}n}\rangle = \mathcal{T}|\tilde{\varphi}_{\mathbf{k}n}\rangle, \tag{44}$$

where the pseudo-wave-function $\tilde{\varphi}_{\mathbf{k}n}$ appears as the image of the $\varphi_{\mathbf{k}n}$ through the transformation $\mathcal{T}$. The PAW method proposes to compute the $\tilde{\varphi}_{\mathbf{k}n}$ instead of the $\varphi_{\mathbf{k}n}$. The equation that is used to compute the $\tilde{\varphi}_{\mathbf{k}n}$ may be obtained by substituting Eq. (44) into Eq. (34). One obtains

$$\tilde{h}|\tilde{\varphi}_{\mathbf{k}n}\rangle = \epsilon_{\mathbf{k}n}\tilde{o}|\tilde{\varphi}_{\mathbf{k}n}\rangle \tag{45}$$

with

$$\tilde{h} = \mathcal{T}^{+}h\mathcal{T}, \tag{46}$$

$$\tilde{o} = \mathcal{T}^{+}\mathcal{T}. \tag{47}$$

For practical calculations, the pseudo-Hamiltonian and overlap operator $\tilde{h}$ and $\tilde{o}$ have been shown in ([29]) and ([30]) to take the simple form

$$\tilde{h} = -\frac{\hbar^2}{2m}\nabla^2 + v_l + \sum_{l\tau}\sum_{LL'}|\tilde{p}_{l\tau L}\rangle D_{LL'}(l\tau)\langle\tilde{p}_{l\tau L'}|, \tag{48}$$

$$\tilde{o} = 1 + \sum_{l\tau}\sum_{LL'}|\tilde{p}_{l\tau L}\rangle Q_{LL'}(l\tau)\langle\tilde{p}_{l\tau L'}| \tag{49}$$

with the PAW strength and overlap parameters given by

$$D_{LL'}(l\tau) = \langle\phi_{l\tau L}|h_\tau|\phi_{l\tau L'}\rangle - \langle\tilde{\phi}_{l\tau L}|\tilde{h}_\tau|\tilde{\phi}_{l\tau L'}\rangle, \tag{50}$$

$$Q_{LL'}(l\tau) = \langle\phi_{l\tau L}|\phi_{l\tau L'}\rangle - \langle\tilde{\phi}_{l\tau L}|\tilde{\phi}_{l\tau L'}\rangle. \tag{51}$$

h_τ and $\tilde{h}_\tau$ are Hamiltonians and pseudo-Hamiltonian for atom τ.

The computational efficiency of the method depends on the choices of the functions $\phi_{l\tau L}$, $\tilde{\phi}_{l\tau L}$ and $\tilde{p}_{l\tau L}$ since they determine how soft will be the potentials in the pseudo-Hamiltonian, and therefore how fast will be the convergence of the plane wave expansion. In a typical calculation using the VASP code [30–32], a cutoff corresponding to $\hbar^2|\mathbf{k}+\mathbf{G}|^2/2m = 520$ eV was sufficient to obtain reliable electronic structures and forces for most of the compounds in the Kyoto Phonon database [4] and Materials Project library [1].

B. The electron-phonon interaction within the PAW formalism

We have shown in Sec. II that the interaction of the electrons with the nuclear degrees of freedom is completely determined by

$$\mathbf{A}^{l\tau}_{\mathbf{k}n,\mathbf{k}'n'} = \langle\varphi_{\mathbf{k}n}| - i\hbar\frac{\partial}{\partial\mathbf{R}_{l\tau}}|\varphi_{\mathbf{k}'n'}\rangle. \tag{52}$$

In particular, they allow to compute the coupling function $g^p(\mathbf{k}n, \mathbf{k}'n', \mathbf{q}j)$.

As eigenfunctions of the Hamiltonians H_e or h, the set of functions Φ_i or $\varphi_{\mathbf{k}n}$ that we used to derive H_n is always complete for any value of the parameters $\mathbf{R}_{l\tau}$. However, in actual calculations, the Hamiltonian is diagonalized using a set of PAW basis functions, $\chi_{\mathbf{k}+\mathbf{G}}$, which is not complete, and not even incomplete in the same manner for different values of the parameters $\mathbf{R}_{l\tau}$. Several of those points were raised by Savrasov in Refs. [33,34] and could be included as an incomplete basis correction in his linear muffin-tin orbitals (LMTO) calculations. Here we shall adapt the derivation to the PAW method.

To make explicit the dependence on atomic positions, the basis functions are written as

$$|\chi_{\mathbf{k}+\mathbf{G}};\mathbf{R}\rangle = \mathcal{T}[\mathbf{R}]|\mathbf{k}+\mathbf{G}\rangle. \tag{53}$$

The Bloch states are expanded as

$$|\varphi_{\mathbf{k}n};\mathbf{R}\rangle = \sum_{\mathbf{G}} a_{\mathbf{k}n}(\mathbf{G};\mathbf{R})|\chi_{\mathbf{k}+\mathbf{G}};\mathbf{R}\rangle \tag{54}$$

and we will need the matrix elements

$$\mathbf{o}_{\mathbf{k}+\mathbf{G},\mathbf{k}'+\mathbf{G}'} = \langle\chi_{\mathbf{k}+\mathbf{G}};\mathbf{R}|\chi_{\mathbf{k}'+\mathbf{G}'};\mathbf{R}\rangle, \tag{55}$$

$$\mathbf{h}_{\mathbf{k}+\mathbf{G},\mathbf{k}'+\mathbf{G}'} = \langle\chi_{\mathbf{k}+\mathbf{G}};\mathbf{R}|h(\mathbf{R})|\chi_{\mathbf{k}'+\mathbf{G}'};\mathbf{R}\rangle. \tag{56}$$

Those matrix elements obviously depend on the atomic positions, however the $\mathbf{R}$ dependence is omitted from the notation for simplicity.

In the PAW basis, the Schrödinger equation, Eq. (34), gives

$$\sum_{\mathbf{G}'}\mathbf{h}_{\mathbf{k}+\mathbf{G},\mathbf{k}'+\mathbf{G}'}a_{\mathbf{k}'n'}(\mathbf{G}';\mathbf{R}) = \epsilon_{\mathbf{k}'n'}(\mathbf{R})\sum_{\mathbf{G}'}\mathbf{o}_{\mathbf{k}+\mathbf{G},\mathbf{k}'+\mathbf{G}'}a_{\mathbf{k}'n'}(\mathbf{G}';\mathbf{R}), \tag{57}$$

$$\sum_{\mathbf{G}\mathbf{G}'}a_{\mathbf{k}n}(\mathbf{G};\mathbf{R})^*(\mathbf{h}_{\mathbf{k}+\mathbf{G},\mathbf{k}'+\mathbf{G}'})a_{\mathbf{k}'n'}(\mathbf{G}';\mathbf{R}) = \delta_{\mathbf{k},\mathbf{k}'}\delta_{n,n'}\epsilon_{\mathbf{k}n}(\mathbf{R}). \tag{58}$$

Taking the derivative with respect to $\mathbf{R}_{l\tau}$, the above equation becomes

$$\begin{aligned}\delta_{\mathbf{k},\mathbf{k}'}\delta_{n,n'}\frac{d\epsilon_{\mathbf{k}n}}{d\mathbf{R}_{l\tau}} &= \sum_{\mathbf{G}\mathbf{G}'}\frac{da_{\mathbf{k}n}(\mathbf{G};\mathbf{R})^*}{d\mathbf{R}_{l\tau}}\mathbf{h}_{\mathbf{k}+\mathbf{G},\mathbf{k}'+\mathbf{G}'}a_{\mathbf{k}'n'}(\mathbf{G}';\mathbf{R})\\ &+\sum_{\mathbf{G}\mathbf{G}'}a_{\mathbf{k}n}(\mathbf{G};\mathbf{R})^*\frac{d\mathbf{h}_{\mathbf{k}+\mathbf{G},\mathbf{k}'+\mathbf{G}'}}{d\mathbf{R}_{l\tau}}a_{\mathbf{k}'n'}(\mathbf{G}';\mathbf{R}) + \sum_{\mathbf{G}\mathbf{G}'}a_{\mathbf{k}n}(\mathbf{G};\mathbf{R})^*\mathbf{h}_{\mathbf{k}+\mathbf{G},\mathbf{k}'+\mathbf{G}'}\frac{da_{\mathbf{k}'n'}(\mathbf{G}';\mathbf{R})}{d\mathbf{R}_{l\tau}}\\ &= \epsilon_{\mathbf{k}'n'}\sum_{\mathbf{G}\mathbf{G}'}\frac{da_{\mathbf{k}n}(\mathbf{G};\mathbf{R})^*}{d\mathbf{R}_{l\tau}}\mathbf{o}_{\mathbf{k}+\mathbf{G},\mathbf{k}'+\mathbf{G}'}a_{\mathbf{k}'n'}(\mathbf{G}';\mathbf{R})\\ &+\sum_{\mathbf{G}\mathbf{G}'}a_{\mathbf{k}n}(\mathbf{G};\mathbf{R})^*\frac{d\mathbf{h}_{\mathbf{k}+\mathbf{G},\mathbf{k}'+\mathbf{G}'}}{d\mathbf{R}_{l\tau}}a_{\mathbf{k}'n'}(\mathbf{G}';\mathbf{R}) + \epsilon_{\mathbf{k}n}\sum_{\mathbf{G}\mathbf{G}'}a_{\mathbf{k}n}(\mathbf{G};\mathbf{R})^*\mathbf{o}_{\mathbf{k}+\mathbf{G},\mathbf{k}'+\mathbf{G}'}\frac{da_{\mathbf{k}'n'}(\mathbf{G}';\mathbf{R})}{d\mathbf{R}_{l\tau}}.\end{aligned} \tag{59}$$

However,

$$\mathbf{A}^{l\tau}_{\mathbf{k}n,\mathbf{k}'n'} = \sum_{\mathbf{G}\mathbf{G}'}a_{\mathbf{k}n}(\mathbf{G};\mathbf{R})^*\mathbf{o}_{\mathbf{k}+\mathbf{G},\mathbf{k}'+\mathbf{G}'}\left(-i\hbar\frac{da_{\mathbf{k}'n'}(\mathbf{G}';\mathbf{R})}{d\mathbf{R}_{l\tau}}\right) + \sum_{\mathbf{G}\mathbf{G}'}a_{\mathbf{k}n}(\mathbf{G};\mathbf{R})^*\langle\chi_{\mathbf{k}+\mathbf{G}};\mathbf{R}| - i\hbar\frac{\partial}{\partial\mathbf{R}_{l\tau}}|\chi_{\mathbf{k}'+\mathbf{G}'};\mathbf{R}\rangle a_{\mathbf{k}'n'}(\mathbf{G}';\mathbf{R}) \tag{60}$$

and

$$\frac{d\mathbf{h}_{\mathbf{k}+\mathbf{G},\mathbf{k}'+\mathbf{G}'}}{d\mathbf{R}_{l\tau}} = \left\langle\frac{d}{d\mathbf{R}_{l\tau}}\chi_{\mathbf{k}+\mathbf{G}};\mathbf{R}\right|h|\chi_{\mathbf{k}'+\mathbf{G}'};\mathbf{R}\rangle + \langle\chi_{\mathbf{k}+\mathbf{G}};\mathbf{R}|\frac{dh}{d\mathbf{R}_{l\tau}}|\chi_{\mathbf{k}'+\mathbf{G}'};\mathbf{R}\rangle + \langle\chi_{\mathbf{k}+\mathbf{G}};\mathbf{R}|h|\frac{d}{d\mathbf{R}_{l\tau}}\chi_{\mathbf{k}'+\mathbf{G}'};\mathbf{R}\rangle. \tag{61}$$

Therefore combining Eqs. (59)–(61) gives

$$\delta_{\mathbf{k},\mathbf{k}'}\delta_{n,n'}\frac{d\epsilon_{\mathbf{k}n}}{d\mathbf{R}_{l\tau}} = \frac{i}{\hbar}(\epsilon_{\mathbf{k}n}-\epsilon_{\mathbf{k}'n'})\mathbf{A}^{l\tau}_{\mathbf{k}n,\mathbf{k}'n'} + \sum_{\mathbf{G}\mathbf{G}'} a_{\mathbf{k}n}(\mathbf{G};\mathbf{R})^*\langle\chi_{\mathbf{k}+\mathbf{G}};\mathbf{R}|\frac{dh}{d\mathbf{R}_{l\tau}}|\chi_{\mathbf{k}'+\mathbf{G}'};\mathbf{R}\rangle a_{\mathbf{k}'n'}(\mathbf{G}';\mathbf{R})$$
$$+\sum_{\mathbf{G}\mathbf{G}'} a_{\mathbf{k}n}(\mathbf{G};\mathbf{R})^*\left\langle\frac{d}{d\mathbf{R}_{l\tau}}\chi_{\mathbf{k}+\mathbf{G}};\mathbf{R}\right|h-\epsilon_{\mathbf{k}'n'}|\chi_{\mathbf{k}'+\mathbf{G}'};\mathbf{R}\rangle a_{\mathbf{k}'n'}(\mathbf{G}';\mathbf{R})$$
$$+\sum_{\mathbf{G}\mathbf{G}'} a_{\mathbf{k}n}(\mathbf{G};\mathbf{R})^*\langle\chi_{\mathbf{k}+\mathbf{G}};\mathbf{R}|h-\epsilon_{\mathbf{k}n}\left|\frac{d}{d\mathbf{R}_{l\tau}}\chi_{\mathbf{k}'+\mathbf{G}'};\mathbf{R}\right\rangle a_{\mathbf{k}'n'}(\mathbf{G}';\mathbf{R}). \tag{62}$$

The PAW basis would be complete, the last two terms would vanish. In forces calculation they are the famous Pulay corrections [35]. In particular, if $\mathbf{k}n=\mathbf{k}'n'$ we recover a formula which may be used in the computations of forces [36],

$$\frac{d\epsilon_{\mathbf{k}n}}{d\mathbf{R}_{l\tau}} = \sum_{\mathbf{G}\mathbf{G}'} a_{\mathbf{k}n}(\mathbf{G};\mathbf{R})^*\left(\frac{d\mathbf{h}_{\mathbf{k}+\mathbf{G},\mathbf{k}+\mathbf{G}'}}{d\mathbf{R}_{l\tau}}-\epsilon_{\mathbf{k}n}\frac{d\mathbf{o}_{\mathbf{k}+\mathbf{G},\mathbf{k}+\mathbf{G}'}}{d\mathbf{R}_{l\tau}}\right)a_{\mathbf{k}n}(\mathbf{G}';\mathbf{R}). \tag{63}$$

However, for $\mathbf{k}n\neq\mathbf{k}'n'$, the left-hand side of the above equation vanishes, and we obtain an equation for $\mathbf{A}^{l\tau}_{\mathbf{k}n,\mathbf{k}'n'}$. From their definitions, the result can be expressed in term of the pseudooperators and pseudo-wave-functions. Using Eqs. (46) and (53), we obtain

$$\mathbf{g}^{l\tau}_{\mathbf{k}n,\mathbf{k}'n'} \equiv -i\frac{\epsilon_{\mathbf{k}n}-\epsilon_{\mathbf{k}'n'}}{\hbar}\mathbf{A}^{l\tau}_{\mathbf{k}n,\mathbf{k}'n'} \tag{64}$$
$$= \sum_{\mathbf{G}\mathbf{G}'} a_{\mathbf{k}n}(\mathbf{G};\mathbf{R})^*\langle\mathbf{k}+\mathbf{G}|\frac{d\tilde{h}}{d\mathbf{R}_{l\tau}}-\epsilon_{\mathbf{k}n}\mathcal{T}^+\frac{d\mathcal{T}}{d\mathbf{R}_{l\tau}}-\epsilon_{\mathbf{k}'n'}\frac{d\mathcal{T}^+}{d\mathbf{R}_{l\tau}}\mathcal{T}|\mathbf{k}'+\mathbf{G}'\rangle a_{\mathbf{k}'n'}(\mathbf{G}';\mathbf{R}) \tag{65}$$
$$= \langle\tilde{\varphi}_{\mathbf{k}n};\mathbf{R}|\frac{d\tilde{h}}{d\mathbf{R}_{l\tau}}-\epsilon_{\mathbf{k}n}\mathcal{T}^+\frac{d\mathcal{T}}{d\mathbf{R}_{l\tau}}-\epsilon_{\mathbf{k}'n'}\frac{d\mathcal{T}^+}{d\mathbf{R}_{l\tau}}\mathcal{T}|\tilde{\varphi}_{\mathbf{k}'n'};\mathbf{R}\rangle. \tag{66}$$

The above equation is the central result of the section. However for a practical calculation one still need to express the derivative of the operators $\tilde{h}$ and $\mathcal{T}$ in term of known PAW quantities. The derivative of the pseudo-Hamiltonian is trivial. From Eq. (48), one obtain

$$\frac{d\tilde{h}}{d\mathbf{R}_{l\tau}} = \frac{dv_l}{d\mathbf{R}_{l\tau}}+\sum_{l'\tau'}\sum_{LL'}|\tilde{p}_{l'\tau'L}\rangle\frac{dD_{LL'}(l'\tau')}{d\mathbf{R}_{l\tau}}\langle\tilde{p}_{l'\tau'L'}|$$
$$+\sum_{LL'}\left|\frac{d}{d\mathbf{R}_{l\tau}}\tilde{p}_{l\tau L}\right\rangle D_{LL'}(l\tau)\langle\tilde{p}_{l\tau L'}|+|\tilde{p}_{l\tau L}\rangle D_{LL'}(l\tau)\left\langle\frac{d}{d\mathbf{R}_{l\tau}}\tilde{p}_{l\tau L'}\right|. \tag{67}$$

To compute the remaining terms, one should first notice that $\mathcal{T}^+\frac{d\mathcal{T}}{d\mathbf{R}_{l\tau}}$ is only nonzero in $\mathcal{S}_{l\tau}$. Then

$$\mathcal{T}^+\frac{d\mathcal{T}}{d\mathbf{R}_{l\tau}} = \left(1+\sum_L|\tilde{p}_{l\tau L}\rangle[\langle\phi_{l\tau L}|-\langle\tilde{\phi}_{l\tau L}|]\right)\frac{d}{d\mathbf{R}_{l\tau}}\sum_{L'}[|\phi_{l\tau L'}\rangle-|\tilde{\phi}_{l\tau L'}\rangle]\langle\tilde{p}_{l\tau L'}| \tag{68}$$
$$= \sum_{LL'}|\tilde{p}_{l\tau L}\rangle\langle\phi_{l\tau L}|\frac{d}{d\mathbf{R}_{l\tau}}(|\phi_{l\tau L'}\rangle\langle\tilde{p}_{l\tau L'}|). \tag{69}$$

However, to obtain a more symmetric result, one might add to the previous equation

$$\frac{d}{d\mathbf{R}_{l\tau}}\sum_L|\tilde{\phi}_{l\tau L}\rangle\langle\tilde{p}_{l\tau L}| = 0. \tag{70}$$

This gives

$$\mathcal{T}^+\frac{d\mathcal{T}}{d\mathbf{R}_{l\tau}} = \sum_{LL'}|\tilde{p}_{l\tau L}\rangle\langle\phi_{l\tau L}|\frac{d}{d\mathbf{R}_{l\tau}}(|\phi_{l\tau L'}\rangle\langle\tilde{p}_{l\tau L'}|)-|\tilde{p}_{l\tau L}\rangle\langle\tilde{\phi}_{l\tau L'}|\frac{d}{d\mathbf{R}_{l\tau}}(|\tilde{\phi}_{l\tau L'}\rangle\langle\tilde{p}_{l\tau L'}|) \tag{71}$$
$$= \sum_{LL'}|\tilde{p}_{l\tau L}\rangle R_{LL'}(l\tau)\langle\tilde{p}_{l\tau L'}|+|\tilde{p}_{l\tau L}\rangle Q_{LL'}(l\tau)\left\langle\frac{d}{d\mathbf{R}_{l\tau}}\tilde{p}_{l\tau L'}\right|, \tag{72}$$

where matrix $Q_{LL'}(l\tau)$ has been defined before at Eq. (51). The matrix $R_{LL'}(l\tau)$ is new. It is defined by

$$R_{LL'}(l\tau) = \left\langle\phi_{l\tau L}\left|\frac{d}{d\mathbf{R}_{l\tau}}\phi_{l\tau L'}\right\rangle-\left\langle\tilde{\phi}_{l\tau L}\left|\frac{d}{d\mathbf{R}_{l\tau}}\tilde{\phi}_{l\tau L'}\right\rangle\right.\right. \tag{73}$$

While the matrix $Q_{LL'}(l\tau)$ is Hermitian in the index L and L', $R_{LL'}(l\tau)$ is anti-Hermitian. Therefore, for the last two terms of Eq. (66), we obtain

$$\epsilon_{\mathbf{k}n}\mathcal{T}^{+}\frac{d\mathcal{T}}{d\mathbf{R}_{l\tau}}+\epsilon_{\mathbf{k}'n'}\frac{d\mathcal{T}^{+}}{d\mathbf{R}_{l\tau}}\mathcal{T}=(\epsilon_{\mathbf{k}n}-\epsilon_{\mathbf{k}'n'})\sum_{LL'}|\tilde{p}_{l\tau L}\rangle R_{LL'}(l\tau)\langle\tilde{p}_{l\tau L'}|+\epsilon_{\mathbf{k}'n'}\sum_{LL'}\left|\frac{d}{d\mathbf{R}_{l\tau}}\tilde{p}_{l\tau L}\right\rangle Q_{LL'}(l\tau)\rangle\tilde{p}_{l\tau L'}|$$
$$+\epsilon_{\mathbf{k}n}\sum_{LL'}|\tilde{p}_{l\tau L}\rangle Q_{LL'}(l\tau)\left\langle\frac{d}{d\mathbf{R}_{l\tau}}\tilde{p}_{l\tau L'}\right|. \tag{74}$$

Finally, collecting the results from Eqs. (66), (67), and (74), we obtain the equation that is implemented numerically in the next section,

$$\mathbf{g}^{l\tau}_{\mathbf{k}n,\mathbf{k}'n'}=\mathbf{g}^{(V),l\tau}_{\mathbf{k}n,\mathbf{k}'n'}+\mathbf{g}^{(D),l\tau}_{\mathbf{k}n,\mathbf{k}'n'}+\mathbf{g}^{(P),l\tau}_{\mathbf{k}n,\mathbf{k}'n'}+\mathbf{g}^{(R),l\tau}_{\mathbf{k}n,\mathbf{k}'n'}, \tag{75}$$

with

$$\mathbf{g}^{(V),l\tau}_{\mathbf{k}n,\mathbf{k}'n'}=\langle\tilde{\varphi}_{\mathbf{k}n};\mathbf{R}|\frac{dv_l}{d\mathbf{R}_{l\tau}}|\tilde{\varphi}_{\mathbf{k}'n'};\mathbf{R}\rangle, \tag{76}$$

$$\mathbf{g}^{(D),l\tau}_{\mathbf{k}n,\mathbf{k}'n'}=\sum_{l'\tau'}\sum_{LL'}\langle\tilde{\varphi}_{\mathbf{k}n};\mathbf{R}|\tilde{p}_{l'\tau'L}\rangle\frac{dD_{LL'}(l'\tau')}{d\mathbf{R}_{l\tau}}\langle\tilde{p}_{l'\tau'L'}|\tilde{\varphi}_{\mathbf{k}'n'};\mathbf{R}\rangle, \tag{77}$$

$$\mathbf{g}^{(P),l\tau}_{\mathbf{k}n,\mathbf{k}'n'}=\sum_{LL'}\langle\tilde{\varphi}_{\mathbf{k}n};\mathbf{R}|\frac{d}{d\mathbf{R}_{l\tau}}\tilde{p}_{l\tau L}\rangle(D_{LL'}(l\tau)-\epsilon_{\mathbf{k}'n'}Q_{LL'}(l\tau))\langle\tilde{p}_{l\tau L'}|\tilde{\varphi}_{\mathbf{k}'n'};\mathbf{R}\rangle$$
$$+\langle\tilde{\varphi}_{\mathbf{k}n};\mathbf{R}|\tilde{p}_{l\tau L}\rangle(D_{LL'}(l\tau)-\epsilon_{\mathbf{k}n}Q_{LL'}(l\tau))\left\langle\frac{d}{d\mathbf{R}_{l\tau}}\tilde{p}_{l\tau L'}\right|\tilde{\varphi}_{\mathbf{k}'n'};\mathbf{R}\right\rangle, \tag{78}$$

$$\mathbf{g}^{(R),l\tau}_{\mathbf{k}n,\mathbf{k}'n'}=-(\epsilon_{\mathbf{k}n}-\epsilon_{\mathbf{k}'n'})\sum_{LL'}\langle\tilde{\varphi}_{\mathbf{k}n};\mathbf{R}|\tilde{p}_{l\tau L}\rangle R_{LL'}(l\tau)\langle\tilde{p}_{l\tau L'}|\tilde{\varphi}_{\mathbf{k}'n'};\mathbf{R}\rangle. \tag{79}$$

Clearly, $\mathbf{g}^{l\tau}_{\mathbf{k}n,\mathbf{k}'n'}$ is Hermitian in the indices $\mathbf{k}n$ and $\mathbf{k}'n'$, $\mathbf{g}^{l\tau}_{\mathbf{k}n,\mathbf{k}'n'}=(\mathbf{g}^{l\tau}_{\mathbf{k}'n',\mathbf{k}n})^{*}$, as it should as a consequence of time reversal symmetry. The coupling functions defined by Eqs. (31) and (33) are obtained from

$$g^{p}(\mathbf{k}n,\mathbf{k}'n',\mathbf{q}j)=\frac{\hbar\omega_{\mathbf{q}j}}{\epsilon_{\mathbf{k}n}-\epsilon_{\mathbf{k}'n'}}\sum_{\tau}\left(\mathbf{g}^{0\tau}_{\mathbf{k}n,\mathbf{k}'n'}\cdot\delta\mathbf{R}^{\mathbf{q}j}_{0\tau}\right)\Delta(\mathbf{q}+\mathbf{k}'-\mathbf{k}), \tag{80}$$

$$g^{e}(\mathbf{k}n,\mathbf{k}'n',\mathbf{q}j)=\sum_{\tau}\left(\mathbf{g}^{0\tau}_{\mathbf{k}n,\mathbf{k}'n'}\cdot\delta\mathbf{R}^{\mathbf{q}j}_{0\tau}\right)\Delta(\mathbf{q}+\mathbf{k}'-\mathbf{k}). \tag{81}$$

IV. IMPLEMENTATION DETAILS

When one run a PAW calculation, the atomic functions $\phi_{l\tau L}$, $\tilde{\phi}_{l\tau L}$, $\tilde{p}_{l\tau L}$, and $Q_{LL'}(l\tau)$ are given as standard inputs, while $\varphi_{\mathbf{k}n}(\mathbf{r})$, $\langle\tilde{p}_{l\tau L}|\tilde{\varphi}_{\mathbf{k}n};\mathbf{R}\rangle$, $v_l(\mathbf{r})$, and $D_{LL'}(l\tau)$ are the standard outputs. To determine $\mathbf{g}^{l\tau}_{\mathbf{k}n,\mathbf{k}'n'}$ the derivatives of those quantities with respect to atomic displacements need to be computed. Our strategy is to perform those derivatives analytically whenever possible, and otherwise from a finite difference approximation obtained by displacing atoms from their equilibrium positions. It is also the strategy that we use to compute phonon spectrums [17] or to compute the anharmonic force constants [18,20] needed to obtain the lattice thermal conductivity [19,20]. In those calculations, a rigorous use of the crystal symmetry is needed to obtain a sufficient accuracy. It will be our philosophy here too. Therefore the atomic displacements used for the finite difference approximations will be exactly those used to obtained the harmonic force constants. This will also ensure the compatibility of the present approach with most of the available phonon codes. In particular, this means the data needed for computing the electron-phonon interactions will be obtained at no more cost than a simple phonon calculation.

A. Derivatives of the local potential

Our goal in this section is to compute

$$\mathbf{g}^{(V),l\tau}_{\mathbf{k}n,\mathbf{k}'n'}=\int d^3r\tilde{\varphi}^{*}_{\mathbf{k}n}(\mathbf{r})\frac{dv_l(\mathbf{r})}{d\mathbf{R}_{l\tau}}\tilde{\varphi}_{\mathbf{k}'n'}(\mathbf{r}) \tag{82}$$

using the same set of atomic displacements that is used to obtain the phonon spectrum in the finite displacement method [17]. In that method one considers a supercell which is the $N_1\times N_2\times N_3$ repetition of a conventional unit cell spanned by the vectors $\mathbf{A}_1$, $\mathbf{A}_2$, $\mathbf{A}_3$. Those lattice vectors are related to the primitive cell lattice vectors $\mathbf{a}_1$, $\mathbf{a}_2$, $\mathbf{a}_3$ through an integer matrix $\mathbf{M}$, $[\mathbf{A}_1,\mathbf{A}_2,\mathbf{A}_3]=[\mathbf{a}_1,\mathbf{a}_2,\mathbf{a}_3]\mathbf{M}$.

In the finite displacement method, the harmonic force constants are computed between each atoms in the supercell using a finite number of displacements $\mathbf{d}_{l\tau,j}$. The first index $l\tau$ label a few atoms in the conventional unit cell, which are called *independent* because all others can be recovered from them using space group operations. The second index j number the displacements performed for atom $l\tau$. The number is chosen such that application of the set of site symmetry operations of atom $l\tau$, $\{\mathbf{S}_{l\tau}\}$, on $\mathbf{d}_{l\tau,j}$ generates three linearly independent displacements. For such displacements, $-\mathbf{d}_{l\tau,j}$ is

then added to list, if not already presents, in order to compte the numerical derivatives using a central difference scheme.

Here we want to compte $dv_l(\mathbf{r})/d\mathbf{R}_{l\tau}$ using the same $\mathbf{d}_{l\tau,j}$. To do that we can use the transformation law of the potential derivative under the space group operations. Indeed, if $\{\mathbf{S}|\mathbf{t}\}$ is a space group operation, then

$$\frac{dv_l(\mathbf{r})}{d\mathbf{R}_{l'\tau'}} = \mathbf{S}\frac{dv_l(\{\mathbf{S}|\mathbf{t}\}^{-1}\mathbf{r})}{d\mathbf{R}_{l\tau}}, \tag{83}$$

where $\mathbf{R}_{l'\tau'}$ is the image of $\mathbf{R}_{l\tau}$ through that space group operation,

$$\mathbf{R}_{l'\tau'} = \{\mathbf{S}|\mathbf{t}\}\mathbf{R}_{l\tau} = \mathbf{S}\mathbf{R}_{l\tau} + \mathbf{t}. \tag{84}$$

If, however, we consider the site symmetry operations around atom $l\tau$, then the transformation law becomes

$$\begin{aligned}(\mathbf{S}_{l\tau}\mathbf{d}_{l\tau,j})\cdot\frac{dv_l(\mathbf{r})}{d\mathbf{R}_{l\tau}} &= \mathbf{d}_{l\tau,j}\cdot\frac{dv_l(\mathbf{S}_{l\tau}^{-1}(\mathbf{r}-\mathbf{R}_{l\tau})+\mathbf{R}_{l\tau})}{d\mathbf{R}_{l\tau}}\\ &\approx \delta v_l(\mathbf{S}_{l\tau}^{-1}(\mathbf{r}-\mathbf{R}_{l\tau})+\mathbf{R}_{l\tau};\mathbf{d}_{l\tau,j}).\end{aligned} \tag{85}$$

In the second line, we defined δv_l to be the selfconsistent change of the local potential, in the supercell, when the atom $l\tau$ is displaced by $\mathbf{d}_{l\tau,j}$. Therefore δv_l can be obtained from standard DFT calculations. Collecting such quantity for the set of displacements $\mathbf{d}_{l\tau,j}$ and for the set of site symmetry operations $\mathbf{S}_{l\tau}$, Eq. (85) gives a linear system of equations for the unknowns $dv_l(\mathbf{r})/d\mathbf{R}_{l\tau}$, at each point $\mathbf{r}$. This system is overdetermined, therefore it is solved using the pseudoinverse method in the same way that we obtain harmonic and anharmonic force constants. For further details see, for example, Eq. (A12) in Ref. [18].

From the output of a supercell calculation, the local potential $v_l(\mathbf{r})$ is known at points $\mathbf{r}$ on a grid $\tilde{\mathbf{x}}_i$ which is uniform and parallel to the vectors $N_1\mathbf{A}_1$, $N_2\mathbf{A}_2$, and $N_3\mathbf{A}_3$. However we want to compute $\mathbf{g}^{(V),l\tau}_{\mathbf{k}n,\mathbf{k}'n'}$ for wave vectors belonging to the first Brillouin zone, and not within the reciprocal cell of the supercell to avoid complicated unfolding procedures. Therefore the wave functions $\tilde{\varphi}_{\mathbf{k}n}(\mathbf{r})$ need to be obtained from a calculation in the primitive cell. Consequently they are known for points $\mathbf{r}$ on a grid $\mathbf{x}_i$ which is parallel to the vectors $\mathbf{a}_1$, $\mathbf{a}_2$, $\mathbf{a}_3$. The grids where the potential and wave functions are known are therefore, in general, different. This prevents from an accurate calculation of the integral in Eq. (82) using a simple accumulation method.

To avoid this grid mismatch problem, and therefore decrease the numerical noise, we first compute the Fourier components of the supercell potential using the usual fast Fourier transform (FFT) algorithm [37]. Those components are then used to compute the values of the potential at the points $\mathbf{x}_i$ where the wave function are known. To obtain those values we used the newly develop nonuniform fast Fourier transform (NFFT) algorithm [38] which allows to compute the value of the potential at arbitrary points from its Fourier components, but still preserving the $N\log N$ scalling of the regular FFT. After this transformation, potential and wave functions are known at the same points, which allows an easy computation of the integral in Eq. (82).

B. Derivatives of the PAW strength

As for the local potential, we compute the derivative of the PAW strength using the finite displacement method in the supercell. To apply the method, we need the transformation law of $dD_{LL'}(l'\tau')/d\mathbf{R}_{l\tau}$ under the space group operations. The strength of the PAW potentials is defined by Eq. (50). Therefore, when atom $l\tau$ is displaced by $\mathbf{d}_{l\tau,j}$, the strength is

$$\begin{aligned}D_{LL'}(l'\tau';\mathbf{d}_{l\tau,j}) = &\langle\phi_{l'\tau'L}|h_\tau[\mathbf{d}_{l\tau,j}]|\phi_{l'\tau'L'}\rangle\\ &-\langle\tilde{\phi}_{l'\tau'L}|\tilde{h}_\tau[\mathbf{d}_{l\tau,j}]|\tilde{\phi}_{l'\tau'L'}\rangle,\end{aligned} \tag{86}$$

where $h_\tau[\mathbf{d}_{l\tau,j}]$ and $\tilde{h}_\tau[\mathbf{d}_{l\tau,j}]$ are the self-consistent Hamiltonians obtained in the displaced configuration.

At first one can assume that the change of the orbitals $\phi_{l\tau L}$ or $\tilde{\phi}_{l\tau L}$ under a space group operation $\{\mathbf{S}|\mathbf{t}\}$, which bring atom $l\tau$ to LT, is implemented using a linear operator $U_{\{\mathbf{S}|\mathbf{t}\}}$ such that

$$U_{\{\mathbf{S}|\mathbf{t}\}}|\phi_{nlm}(l\tau)\rangle = \sum_{M=-l}^{l}|\phi_{nlM}(LT)\rangle\Delta^l_{Mm}, \tag{87}$$

where the matrix Δ^l_{Mm} is unitary with respect to the indices M and m. Since the Hamiltonian transforms according to

$$h'_{L'T'} = U_{\{\mathbf{S}|\mathbf{t}\}}h_{l'\tau'}U^+_{\{\mathbf{S}|\mathbf{t}\}}, \tag{88}$$

using $\mathbf{d}_{LT,j} = \mathbf{S}\mathbf{d}_{l\tau,j}$, we obtain

$$\begin{aligned}&D_{nlm,n'l'm'}(l'\tau';\mathbf{d}_{l\tau,j})\\ &\quad=\sum_{M=-l}^{l}\sum_{M'=-l'}^{l'}\Delta^{l+}_{mM}D_{nlM,n'l'M'}(L'T';\mathbf{d}_{LT,j})\Delta^{l'}_{M'm'}.\end{aligned} \tag{89}$$

In matrix form, this is written as

$$D(L'T';\mathbf{d}_{LT,j}) = \Delta D(l'\tau';\mathbf{d}_{l\tau,j})\Delta^+. \tag{90}$$

In the limit of small displacements, Taylor expanding this equation gives

$$\mathbf{S}\mathbf{d}_{l\tau,j}\cdot\frac{\partial D(L'T')}{\partial\mathbf{R}_{LT}} = \Delta\left(\mathbf{d}_{l\tau,j}\cdot\frac{\partial D(l'\tau')}{\partial\mathbf{R}_{l\tau}}\right)\Delta^+. \tag{91}$$

The right-hand side of the above equation,

$$\delta_{\Delta_{l\tau,j}}D(l'\tau') \equiv \Delta\left(\mathbf{d}_{l\tau,j}\cdot\frac{\partial D(l'\tau')}{\partial\mathbf{R}_{l\tau}}\right)\Delta^+ \tag{92}$$

$$\approx \Delta(D(l'\tau';\mathbf{d}_{l\tau,j}) - D(l'\tau'))\Delta^+, \tag{93}$$

can be computed from the output of the PAW calculations. Therefore collecting those results for the set of displacements $\mathbf{d}_{l\tau,j}$ and site symmetry operations of atom $l\tau$, we obtain an overdetermined set of equations for $\partial D(L'T')/\partial\mathbf{R}_{LT}$ which is solved using the pseudoinverse method as in the previous section.

From a practical point of view, to implement this method, the matrix Δ needs to be known. Its expression is derived in Appendix C.

C. Derivatives of projectors

The projectors $\langle\tilde{p}_{l\tau L}|\tilde{\varphi}_{\mathbf{k}n};\mathbf{R}\rangle$ which are needed to compute $\mathbf{g}^{(P),l\tau}_{\mathbf{k}n,\mathbf{k}'n'}$ are standard outputs of the PAW calculations. They can be obtained from the expansion of the exponentials in

Eq. (36) into Bessel functions and spherical harmonics using the Rayleigh formula. Thanks to our definition of real spherical harmonics, this expansion remains the same for complex and real spherical harmonics. Therefore we have

$$\langle \tilde{p}_{l\tau L} | \tilde{\varphi}_{\mathbf{k}n}; \mathbf{R} \rangle = \sum_{\mathbf{G}} a_{\mathbf{k}n}(\mathbf{G}) e^{i(\mathbf{k}+\mathbf{G})\cdot\mathbf{R}_{l\tau}} \times \int d^3r\, P_{nl}(r) S_{lm}(\hat{r}) \frac{e^{i(\mathbf{k}+\mathbf{G})\cdot\mathbf{r}}}{\sqrt{\Omega}} \quad (94)$$

with the integral computed as explained above. $P_{nl}(r)$ is the radial function defining the projector.

The projector derivatives needed to compute $\mathbf{g}^{(P),l\tau}_{\mathbf{k}n,\mathbf{k}'n'}$ can be written in a similar way. A term by term derivative of the above equation gives

$$\left\langle \frac{d}{d\mathbf{R}_{l\tau}} \tilde{p}_{l\tau L} \middle| \tilde{\varphi}_{\mathbf{k}n}; \mathbf{R} \right\rangle = \sum_{\mathbf{G}} i(\mathbf{k}+\mathbf{G}) a_{\mathbf{k}n}(\mathbf{G}) e^{i(\mathbf{k}+\mathbf{G})\cdot\mathbf{R}_{l\tau}} \times \int d^3r\, P_{nl}(r) S_{lm}(\hat{r}) \frac{e^{i(\mathbf{k}+\mathbf{G})\cdot\mathbf{r}}}{\sqrt{\Omega}}, \quad (95)$$

which can be computed using the same procedure than the projectors themselves.

D. Derivatives of (pseudo)orbitals

In this section, we want to compute the matrix $R_{LL'}(l\tau)$ defined at Eq. (73). This involves the calculation of the scalar product

$$\left\langle \phi_{l\tau L_1} \middle| \frac{d}{dR_{l\tau}} \phi_{l\tau L_2} \right\rangle = -\int d^3r\, \phi^*_{n_1 l_1 m_1}(\mathbf{r}) \nabla \phi_{n_2 l_2 m_2}(\mathbf{r}), \quad (96)$$

for orbitals and pseudo-orbitals. The angular part of the scalar product can be computed analytically, while the radial part requires to take the derivative and integrate the radial functions $R_{nl}(r)$ on a logarithmic grid in the atomic sphere around each atom. Those calculations are straightforward but lengthy, therefore they have been summarized in the Appendices D and B.

V. RESULTS

In the previous sections, we obtained the formulas to compute the electron-phonon coupling function using the PAW method. In this section we apply our implementation using the VASP code to some simple systems, aluminium and diamond, to test the accuracy and convergence of the method. For the conventional cells, the lattice parameters we obtain are respectively $a_{Al} = 4.04$ Å and $a_C = 3.57$ Å, and the electronic and phonon band structures for both those systems are shown in Figs. 1 and 4. Both systems are computed using the Perdew-Burke-Ernzerhof (PBE) exchange correlation functional [39], with an energy cutoff of 600 eV. The phonon states are computed using the finite displacement method using different supercell sizes. As shown on the figures below, $2 \times 2 \times 2$, $3 \times 3 \times 3$, and $4 \times 4 \times 4$ multiples of the conventional cubic cells are considered. The corresponding reciprocal cells are sampled with respectively $6 \times 6 \times 6$, $4 \times 4 \times 4$, and $3 \times 3 \times 3$ uniformly distributed grid points.

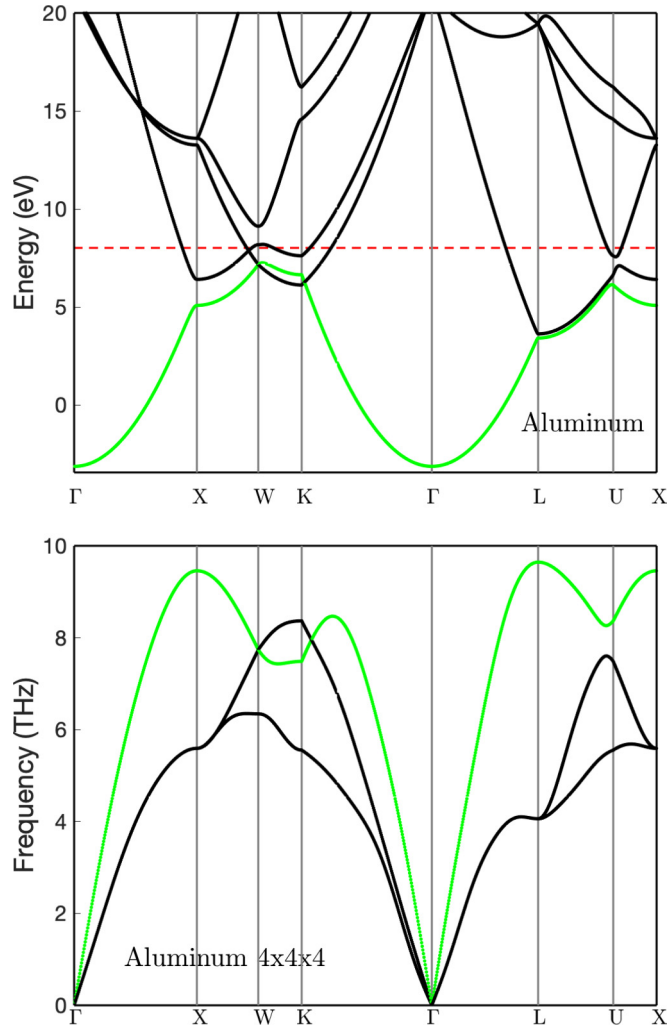

FIG. 1. Electron (top) and phonon (bottom) band structures for aluminium. The Fermi level is shown using a red dashed line. The results shown for phonons are obtained using the $4 \times 4 \times 4$ supercell. The bands in green correspond to the states involved in the calculation of the electron-phonon coupling function shown in Fig. 2.

A. Aluminium

To plot the coupling function $g^e(\mathbf{k}n, \mathbf{k}'n', \mathbf{q}j)$, we may fix the initial electronic states $\varphi_{\mathbf{k}'n'}$, the phonon band index j, the band of the final electronic state n, and discuss the probability amplitude for an electron in state $\varphi_{\mathbf{k}'n'}$, when scattered by a phonon in mode $\mathbf{q}j$, to end up in state $\varphi_{\mathbf{k}n}$ with $\mathbf{k} = \mathbf{k}' + \mathbf{q} + \mathbf{G}$. However, the electron and phonon states may be degenerate. In this case, the quantity that we consider is

$$|g|^2 = \frac{1}{g_n g_j g_{n'}} \sum_n \sum_j \sum_{n'} |g^e(\mathbf{k}n, \mathbf{k}'n', \mathbf{q}j)|^2, \quad (97)$$

where the sums run over the degenerate bands, and g_n, $g_{n'}$ and g_j are the number of those bands for electrons and phonons, respectively.

The result of such calculation is shown in Fig. 2 for aluminium, for the three supercell sizes we consider, and for selected electron and phonon states which are easily extracted

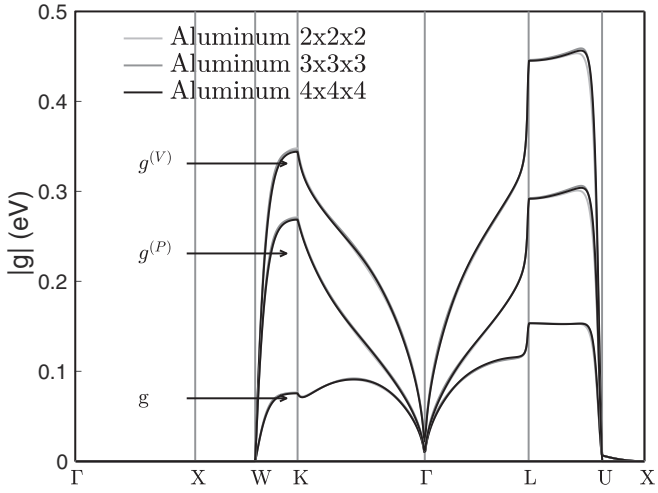

FIG. 2. Electron-phonon coupling functions g^e for aluminium. The electron and phonon bands and wave vectors are selected as described in the text. The graphs shows the different contributions to the total coupling functions. The notations are defined in Eqs. (76)–(79). The different gray intensities correspond to different supercell sizes.

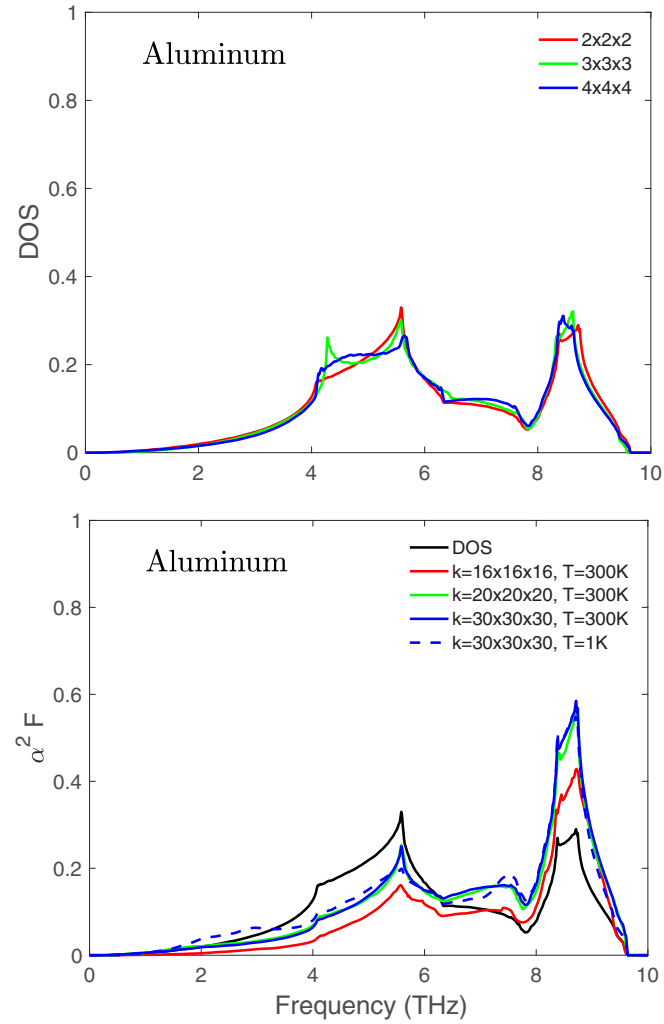

FIG. 3. (Top) Phonon density of states per degree of freedom for different supercell sizes. (Bottom) Eliashberg function at 1 and 300 K, for several sampling of the Brillouin zone. The $2 \times 2 \times 2$ supercell is used for the calculation. The Eliashberg function at 1 K is shown using dashed line, and the values at 300 K with continuous lines.

from the numerical data. For the initial state, we consider the first unoccupied states at the zone center. Its energy ($\epsilon_{\mathbf{k}'n'} \approx 20$ eV) is triply degenerates, and the eigenstates belongs to the irreducible representation Γ'_{25}. We take the final state to be the lowest energy state in our energy windows, except along the WK direction where we merge with the Σ_1 band of the ΓK direction. For the phonon state, we select the highest frequency state, except along the WK direction where we merge with the $(1/\sqrt{2}, 1/\sqrt{2}, 0)$ eigenstate of the ΓK direction. They are represented with green lines in Fig. 1.

Figure 2 shows the result of our calculations for the different supercell sizes that we have considered. The results are almost superimposed. This proves that the perturbation created in the *potential* is localized enough for the electron-phonon coupling to be computed using the finite displacement method. Figure 2 shows also the contributions of $g^{(V)}$ and $g^{(P)}$ to the total coupling function g, as defined by Eqs. (75)–(79). $g^{(D)}$ and $g^{(R)}$ are negligibly small and therefore are not shown. May be surprisingly, $|g|$ is significantly less than the sum of $|g^{(V)}|$ and $|g^{(P)}|$, denoting an *out of phase* behavior. The electron-phonon coupling seems to be zero along the Γ-X-W path. This can be explained as follow. Considering a nearest-neighbor interactions model, for the branch that we consider, the phonon eigenvectors are along the axes of the cube in the ΓX and XW directions. In particular, $\mathbf{e}_1^{\mathbf{q}3} = (1 \quad 0 \quad 0)^t$. Therefore

$$g^e(\mathbf{k}n, \mathbf{k}'n', \mathbf{q}j) \propto \langle \tilde{\varphi}_{\mathbf{k}n} | \frac{d\tilde{V}}{dx} | \tilde{\varphi}_{\mathbf{k}'n'} \rangle,$$
$$\propto \langle \tilde{\varphi}_{\mathbf{k}n} | (|S_{11}\rangle\langle S_{00}| + |S_{00}\rangle\langle S_{11}|) | \tilde{\varphi}_{\mathbf{k}'n'} \rangle$$

where in the second line, we represent the derivative of the potential as an electric-dipole operator in the x direction. The initial states belongs to the Γ'_{25} representation, and therefore transforms like xy, yz, and zx, which are orthogonal to S_{00} and S_{11} and therefore gives a vanishing electron-phonon coupling. The final state belongs to the Δ_1 representation along ΓX and to Z_3 along XW, whose basis functions transform like x. Therefore a zero coupling can only result from a choice of initial state, as in the present case.

In Fig. 3 (down), we consider the isotropic Eliashberg function [40,41],

$$\alpha^2 F(\omega) = \frac{1}{2\pi\hbar N(\mu)} \frac{1}{N} \sum_{\mathbf{q}j} \frac{\gamma_{\mathbf{q}j}}{\omega_{\mathbf{q}j}} \delta(\omega - \omega_{\mathbf{q}j}),$$

where $N(\mu)$ is the electronic density of states, per spin and per atom, at the chemical potential μ, and $\gamma_{\mathbf{q}j} = 1/2\tau_{\mathbf{q}j}$, the phonon linewidth. Our definition may be slightly different from previous implementations [12], since we allow $N(\mu)$ and $\tau_{\mathbf{q}j}$ to depend on temperature. The tetrahedron method is used to perform the Brillouin zone integration in the previous equation, and in Eq. (32) as well to get the phonon lifetime. We used the $2 \times 2 \times 2$ supercell to perform the calculation. We observe that the Eliashberg function is converged for a

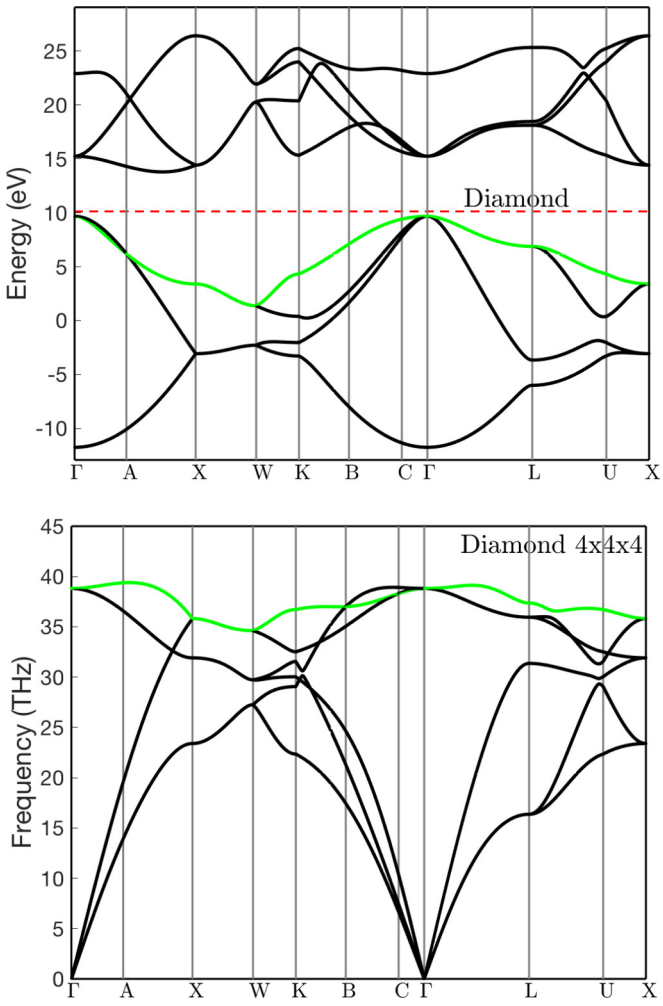

FIG. 4. Electron (top) and phonon (bottom) bands structure for diamond. The Fermi level is shown using a red dashed line. The results shown for phonons are obtained using the $4 \times 4 \times 4$ supercell.

$30 \times 30 \times 30$ sampling of the Brillouin zone, and take values which are very close for 1 K and 300 K. From Fig. 3 (top), we notice that the phonon spectrum itself is difficult to converges with respect to the supercell size. Indeed, for small supercell size, the Van Hove singularities seem to be poorly described [42].

Using the Eliashberg function, one can compute the average coupling strength λ,

$$\lambda = 2 \int_0^{+\infty} \frac{d\omega}{\omega} \alpha^2 F(\omega), \tag{98}$$

which allow to obtain an estimate for the critical temperature T_c of BCS superconductors using the modified McMillan formula [43,44], or, in a first approximation, to estimate to electron lifetime τ_e due to phonon scattering, around the Fermi energy [45]. We obtain 0.37 at 300 K, which is in good agreement with Ref. [12] (0.37), and 0.40 at 1 K, which is lower than 0.44, the value reported in Ref. [34]. In both the previous references the local density approximation (LDA) is used for the exchange correlation potential. If we use the LDA to compute the electron-phonon interaction within our implementation, we obtain 0.45 at 1 K, and 0.36 at 300 K, in good agreement with the published results.

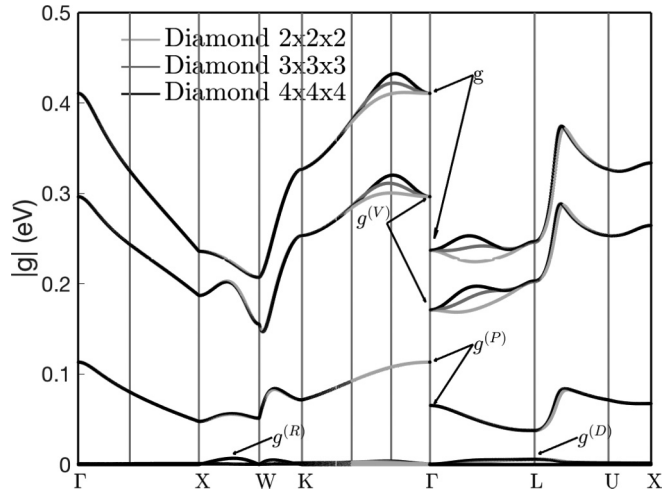

FIG. 5. Electron-phonon coupling functions g^e for diamond. The graphs shows the different contributions to the total coupling functions. The notations are defined in Eqs. (76)–(79). The different colours correspond to different supercell sizes.

B. Diamond

For diamond, we chose the initial electronic state to be the state at the top of the valance band at the zone center. This state is degenerated three times, and belongs to the Γ'_{25} representation. The phonon path is shown in Fig. 4, and the band index correspond to the green line in this figure. We have chosen the highest optical band, except in the ΓK direction where we have chosen the Σ_1 band. The final electronic states are taken at the top of the valence band, except in the ΓX direction where we have considered the Δ_5 band which is two times degenerated.

$|g|$ is plotted in Fig. 5, and takes values around 0.3 eV along the path we have chosen, in good agreement with Ref. [13]. The results seem to be well converged with respect to supercell size in most directions. Nevertheless the convergence appears to be more difficult in the ΓK and ΓL directions.

In the ΓL direction, the eigenvectors of the longitudinal optical mode (LO) that we are considering can be written as [46]

$$\mathbf{e}_1^{\mathbf{q}LO} = -\frac{1}{\sqrt{2}} \frac{\mathbf{q}}{q}, \tag{99}$$

$$\mathbf{e}_2^{\mathbf{q}LO} = \frac{1}{\sqrt{2}} \exp\left(i\phi_{\mathrm{LO}}(\mathbf{q})\right) \frac{\mathbf{q}}{q}, \tag{100}$$

In Fig. 6 (top), we have plotted the phase angle $\phi_{\mathrm{LO}}(\mathbf{q})$ and the phonon frequency $\omega_{\mathrm{LO}}(\mathbf{q})$ along the ΓL direction for different supercell sizes. The phase angle we obtain is, of course, the same for the different sizes. However the frequency is poorly converged. In Fig. 6 (bottom), the derivative of the potential, in the [111] direction, with respect to the position of the second carbon atom, is plotted for the different supercell sizes. It appears to be well converged already for the $2 \times 2 \times 2$ supercell. Therefore the more difficult convergence of $|g|$ in

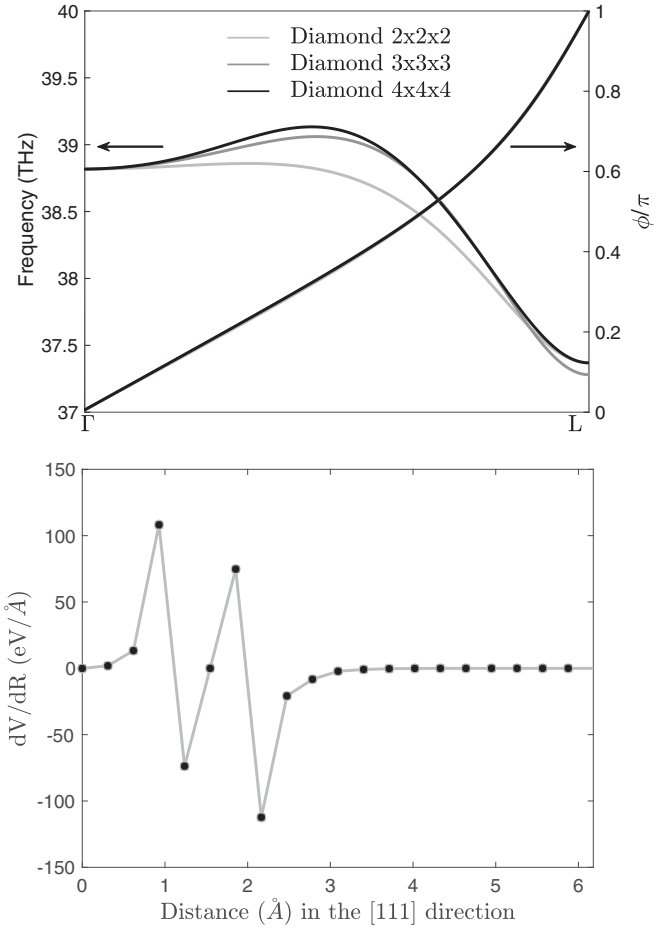

FIG. 6. Frequency and phase angle of the longitudinal optical mode of diamond along the ΓL direction computed using $2 \times 2 \times 2$, $3 \times 3 \times 3$, and $4 \times 4 \times 4$ supercells. The derivative of the local potential with respect to atom at [1/4 1/4 1/4] is also shown for the three supercell sizes.

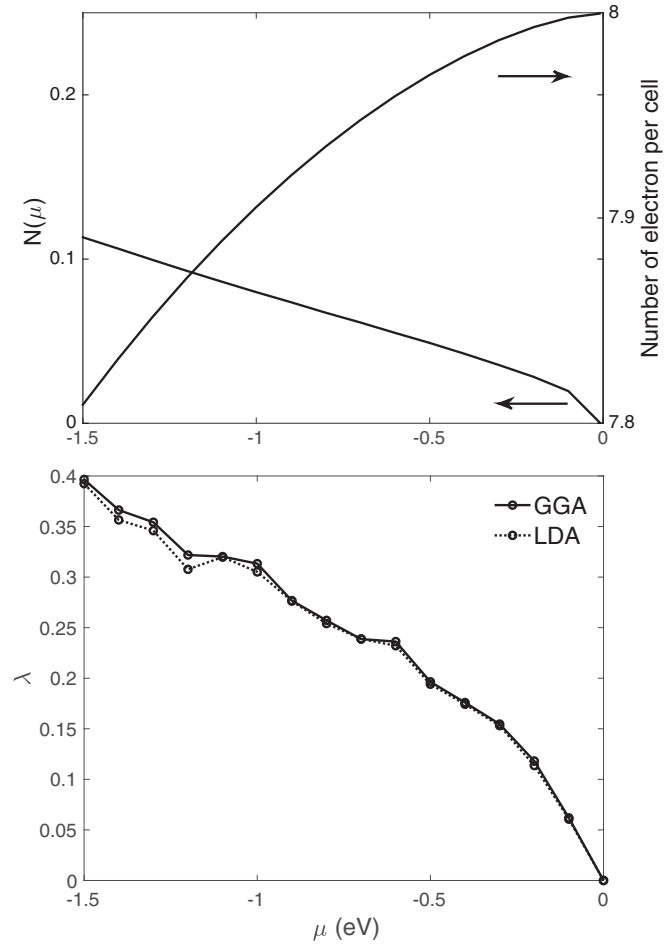

FIG. 7. (Top) Density of states and number of doping electrons as functions of the chemical potential. (Bottom) Average electron-phonon coupling as a function of the chemical potential at 300 K. Chemical potential is measured with respect to the valence-band maximum. For those computations, we used the $2 \times 2 \times 2$ supercell and a $40 \times 40 \times 40$ sampling of the Brillouin zone.

the ΓK and ΓL directions can be attributed to the phonon band structure itself, and understood as a limitation of supercell approach.

In Fig. 5, $|g|$ is decomposed into the different contributions coming from the PAW method. $g^{(D)}$ and $g^{(R)}$ are small, but not negligible however. Moreover, $|g|$ is almost the sum of $|g^{(V)}|$, $|g^{(P)}|$, $|g^{(D)}|$, and $|g^{(R)}|$, which means that those components are roughly *in phase*, unlike the aluminium case.

In Figs. 7 and 8, we consider p-doped diamond in the rigid band approximation, at 300 K, and compute several quantities as functions of the chemical potential. The $2 \times 2 \times 2$ supercell is used for those computations, and a $40 \times 40 \times 40$ mesh is used to sample the Brillouin zone. We consider chemical potentials in the range from ϵ_F to $\epsilon_F - 1.5$ eV; this correspond to a doping up to 0.2 holes per primitive unit cell.

In Fig. 7 (bottom), we observe that between ϵ_F and $\epsilon_F - 1.5$ eV the average electron-phonon coupling increase from 0 to 0.4 as the doping is increased. Our results follow the behavior of the computations reported in Ref. [47], and our values for λ are in reasonable agreement with those of the above mentioned reference, which uses the LDA. We performed the computations with both the GGA and the LDA for the exchange correlation potential; they give very similar results.

The Eliashberg function and the reciprocal phonon lifetime are plotted in Figs. 8 and 9 for several chemical potentials, from light to heavy doping. As we move closer to the top of the valence band, the Eliashberg function localises around the optical mode of the phonon spectrum as a result of decreased values for $1/\tau_{\mathbf{q}j}$ over the rest of the spectrum. From Eq. (32), in the limit of low temperatures, together with the delta functions which take care of the conservation of energy and momentum, this is a consequence of the factor $(\theta(\epsilon_F - \epsilon_{\mathbf{k}'n'}) - \theta(\epsilon_F - \epsilon_{\mathbf{k}n}))$ which insures that the states $\mathbf{k}'n'$ and $\mathbf{k}n$ must be occupied and unoccupied, respectively. When ϵ_F is at the top of the valence band, due to the large electronic band gap of diamond, $E_g^{\mathrm{PBE}} = 4.1$ eV, no phonon have enough energy $\hbar\omega_{\mathbf{q}j} < \hbar\omega_M = 0.16$ eV to find an empty state. However, when ϵ_F is close but below the top of the valence band (ϵ_M), electrons may be scattered to empty states by phonons with wave vectors $q \lessapprox 2\sqrt{(2m/\hbar^2)(\epsilon_M - \epsilon_F)} + 2mc/\hbar$ if we are considering acoustic phonons with group

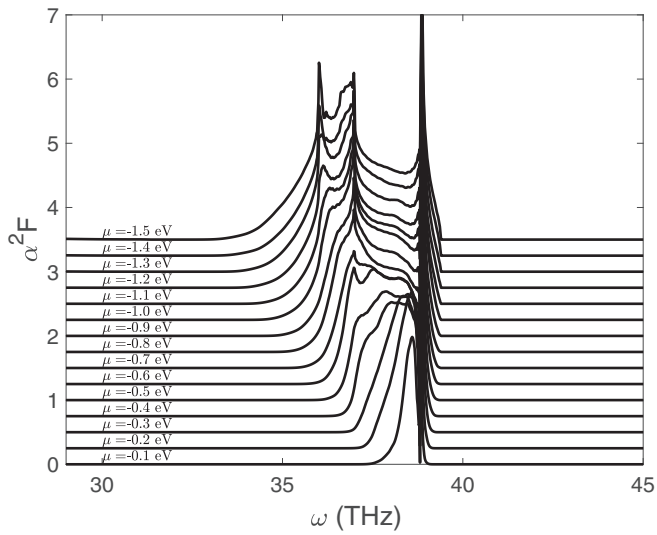

FIG. 8. Eliashberg function a as functions of the phonon frequency for different chemical potentials, from 0.1 to 1.5 eV, every 0.1 eV, below the valence-band maximum. The curves are shifted upward by 0.25 from the previous one for clarity.

velocity c, or $q \lessapprox \sqrt{(2m/\hbar^2)\hbar\omega_M}$ if we are considering optical phonons. For small enough doping, the number of available phonons is therefore larger in the optical bands than in the acoustics bands, as observed in Fig. 8.

VI. CONCLUSIONS

In this work, we have developed a formalism based on the PAW method to compute electron-phonon interactions from finite displacements.

Our approach has been implemented as a computer code, and has been used to computed several quantities. It is found that the electron-phonon interactions g decompose into four contributions inherited from the PAW transformation. The first $g^{(V)}$ involves the derivative of the local part of the potential, and the second $g^{(P)}$ the derivative of the projector functions. They are the two main contributions to g in the examples we have tested. The remaining two contributions $g^{(D)}$ and $g^{(R)}$ involve the derivative of the strength of the non local part of the potential, and the derivative of the local orbitals. They are small in the examples we have considered. While the computation of $g^{(P)}$ is simple and fast in reciprocal space, the computation of $g^{(V)}$ is performed in real space and requires subtile grid techniques to be efficient and accurate. The use of different exchange correlation functionals is therefore straightforward, as shown in the results section. It is found that the derivatives of the local and non local potentials are quickly convergent with respect to the supercell size. This guaranties the applicability of our approach if the finite displacement method can be used to obtain the phonon spectrum. Moreover, for the examples we have considered, we have shown that our strategy allows computing the Eliashberg function and the phonon lifetime without the need for an interpolation method, or a Wannier transformation, to perform the Brillouin zone integration. If this is confirmed for more complicated systems this will be an advantage to perform high-throughput calculations. However more testing is required, and this will be the purpose of future works.

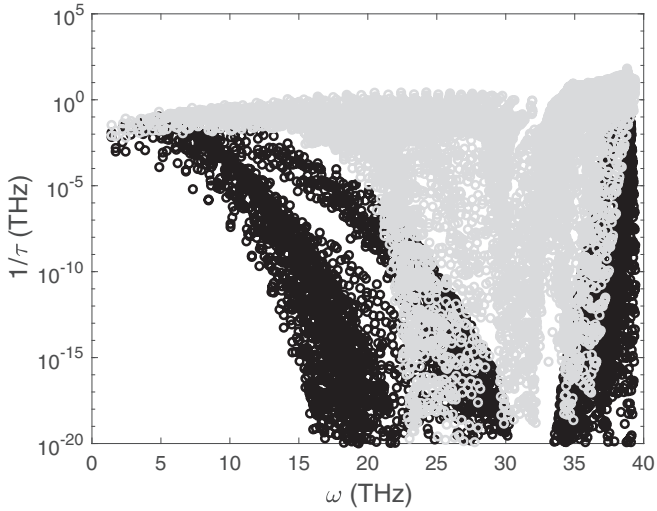

FIG. 9. Phonon lifetime as a function of the phonon frequency for two different values of the chemical potentials. The $\mu = -0.1$ eV value is shown with black circles and the $\mu = -1.5$ eV value using light gray circles.

APPENDIX A: PHONONS

When in Eq. (11) the potential energy is expanded to second order in the atomic displacements around the equilibrium positions $\mathbf{R}^0_{l\tau}$, the Hamiltonian becomes

$$[H_{\mathrm{BO}}]_{ii} \approx \sum_{l\tau\alpha} -\frac{\hbar^2}{2M_\tau}\frac{\partial^2}{\partial R^2_{l\tau\alpha}} + \frac{1}{2}\sum_{l\tau\alpha}\sum_{l'\tau'\alpha'} \delta R_{l\tau\alpha}\frac{\partial^2 E_i}{\partial R^0_{l\tau\alpha}\partial R^0_{l'\tau'\alpha'}}\delta R_{l'\tau'\alpha'} \quad \text{(A1)}$$

$$= \sum_{\mathbf{q}j}\hbar\omega_{\mathbf{q}j}\left(a^+_{\mathbf{q}j}a_{\mathbf{q}j} + \frac{1}{2}\right), \quad \text{(A2)}$$

where we have used the notation $\delta R_{l\tau\alpha} = R_{l\tau\alpha} - R^0_{l\tau\alpha}$. In the last line, the phonon Hamiltonian has been rewritten using the annihilation and creation operators for a phonon with wave vector $\mathbf{q}$ and band index j. They are defined by

$$a_{\mathbf{q}j} = \sqrt{\frac{\omega_{\mathbf{q}j}}{2\hbar}}\sum_{l\tau\alpha}\frac{e^{-i\mathbf{q}\cdot\mathbf{l}}e^{\mathbf{q}j*}_{\tau\alpha}}{\sqrt{N}} \times\left(\sqrt{M_\tau}\delta R_{l\tau\alpha} + \frac{i}{\omega_{\mathbf{q}j}}\frac{1}{\sqrt{M_\tau}}\left(-i\hbar\frac{\partial}{\partial R_{l\tau\alpha}}\right)\right), \quad \text{(A3)}$$

$$a^+_{\mathbf{q}j} = \sqrt{\frac{\omega_{\mathbf{q}j}}{2\hbar}}\sum_{l\tau\alpha}\frac{e^{i\mathbf{q}\cdot\mathbf{l}}e^{\mathbf{q}j}_{\tau\alpha}}{\sqrt{N}} \times\left(\sqrt{M_\tau}\delta R_{l\tau\alpha} - \frac{i}{\omega_{\mathbf{q}j}}\frac{1}{\sqrt{M_\tau}}\left(-i\hbar\frac{\partial}{\partial R_{l\tau\alpha}}\right)\right), \quad \text{(A4)}$$

where $\omega^2_{\mathbf{q}j}$ and $e^{\mathbf{q}j}_{\tau\alpha}$ are the eigenvalues and eigenvectors of the dynamical matrix

$$D_{\tau\alpha,\tau'\alpha'}(\mathbf{q}) = \sum_{l'} e^{i\mathbf{q}\cdot\mathbf{l}'} \frac{1}{\sqrt{M_\tau}} \frac{\partial^2 E_i}{\partial R^0_{0\tau\alpha} \partial R^0_{l'\tau'\alpha'}} \frac{1}{\sqrt{M_{\tau'}}}. \tag{A5}$$

For further reference we recall that the creation and annihilation operators fulfill the canonical commutation relations

$$[a_{\mathbf{q}j}, a^+_{\mathbf{q}'j'}] = \delta_{\mathbf{q},\mathbf{q}'}\delta_{jj'}, \quad [a_{\mathbf{q}j}, a_{\mathbf{q}'j'}] = [a^+_{\mathbf{q}j}, a^+_{\mathbf{q}'j'}] = 0, \tag{A6}$$

which gives the eigenvalues and eigenstates of $[H_{\mathrm{BO}}]_{ii}$,

$$E_{\{n_{\mathbf{q}j}\}} = \sum_{\mathbf{q}j} \hbar\omega_{\mathbf{q}j}\left(n_{\mathbf{q}j} + \frac{1}{2}\right), \tag{A7}$$

$$|\{n_{\mathbf{q}j}\}\rangle = \prod_{\mathbf{q}j} \frac{(a^+_{\mathbf{q}j})^{n_{\mathbf{q}j}}}{\sqrt{n_{\mathbf{q}j}!}}|0\rangle. \tag{A8}$$

$\{n_{\mathbf{q}j}\}$ is the list of phonon occupation number $n_{\mathbf{q}j} = 0, 1, 2, \ldots$ over the first Brillouin zone, and $|0\rangle$ is the product of $3N_aN$ ground states of one dimensional linear harmonic oscillators.

Strictly speaking all of the above phonon properties depends on the particular electronic states i that we consider. For example we should write $\omega^i_{\mathbf{q}j}$ instead of $\omega_{\mathbf{q}j}$. This is however not consider in the present paper.

APPENDIX B: SPHERICAL HARMONICS AND LEGENDRE FUNCTIONS

The complex spherical harmonics we use are defined by

$$Y_{lm}(\theta,\varphi) = (-1)^m N_{lm} P_{lm}(\cos\theta) e^{im\varphi}, \quad l \geqslant 0, \quad -l \leqslant m \leqslant l,$$

$$N_{lm} = \sqrt{\frac{2l+1}{4\pi}\frac{(l-m)!}{(l+m)!}},$$

$$P_{lm}(x) = (1-x^2)^{m/2}\frac{d^m}{dx^m}P_l(x), \quad l \geqslant 0, m \geqslant 0,$$

$$P_l(x) = \frac{1}{2^l l!}\frac{d^l}{dx^l}(x^2-1)^l.$$

P_l are the Legendre functions, and P_{lm} the associated Legendre functions. The associated Legendre functions with negative values of l and/or m are obtained from

$$P_{l-|m|}(x) = (-1)^{|m|}\frac{(l-|m|)!}{(l+|m|)!}P_{l|m|}(x),$$

$$P_{-lm}(x) = P_{l-1m}(x).$$

Using these equations, the real spherical harmonics defined by Eq. (C4) can be written as

$$S_{l,m}(\hat{\mathbf{r}}) = N_{l|m|}P_{l|m|}(\cos\theta) \times \begin{cases} \sqrt{2}\cos(|m|\varphi) & \text{if} \quad m > 0 \\ 1 \quad \text{if} \quad m = 0 \\ \sqrt{2}\sin(|m|\varphi) & \text{if} \quad m < 0 \end{cases} \tag{B1}$$

$$\equiv N_{l|m|}P_{l|m|}(\cos\theta) \times c_m(\varphi). \tag{B2}$$

The associated Legendre functions are shown to fulfill a few useful formulas. One has the recurrence relations [48],

$$\sqrt{1-x^2}\frac{d}{dx}P_{lm} = \frac{1}{2}[P_{lm+1}(x) - (l+m)(l-m+1)P_{lm-1}(x)],$$

$$\frac{1}{\sqrt{1-x^2}}P_{lm}(x) = \frac{1}{2m}[P_{l+1m+1} + (l-m+1)(l-m+2)P_{l+1m-1}(x)],$$

$$\sqrt{1-x^2}P_{lm}(x) = \frac{1}{2l+1}[P_{l+1,m+1}(x) - P_{l-1,m+1}(x)],$$

$$\sqrt{1-x^2}P_{lm}(x) = \frac{1}{2l+1}[(l+m-1)(l+m)P_{l-1,m-1}(x) - (l-m+1)(l-m+2)P_{l+1,m-1}(x)],$$

$$xP_{lm}(x) = \frac{l+m}{2l+1}P_{l-1,m}(x) + \frac{l-m+1}{2l+1}P_{l+1,m}(x),$$

and the multiplication formula,

$$P_{l_1m_1}(x)P_{l_2m_2}(x) = \sum_{l=|l_1-l_2|}^{l_1+l_2} (-1)^{m_1+m_2}(2l+1)\sqrt{\frac{(l-m_1-m_2)!(l_1+m_1)!(l_2+m_2)!}{(l+m_1+m_2)!(l_1-m_1)!(l_2-m_2)!}} \times \begin{pmatrix} l_1 & l_2 & l \\ 0 & 0 & 0 \end{pmatrix}\begin{pmatrix} l_1 & l_2 & l \\ m_1 & m_2 & -m_1-m_2 \end{pmatrix} P_{lm_1+m_2}(x) \tag{B3}$$

$$\equiv \sum_{l=|l_1-l_2|}^{l_1+l_2} g^l_{l_1m_1,l_2m_2} P_{lm_1+m_2}(x). \tag{B4}$$

where the Wigner 3-j symbols appearing in this equation can be computed from [49]

$$\begin{pmatrix} l_1 & l_2 & l_3 \\ m_1 & m_2 & m_3 \end{pmatrix} = \delta_{m_1+m_2+m_3,0}(-1)^{l_1-l_2-m_3}\sqrt{(l_1+l_2-l_3)!(l_1-l_2+l_3)!(-l_1+l_2+l_3)!} \tag{B5}$$

$$\times \sqrt{\frac{(l_1+m_1)!(l_1-m_1)!(l_2+m_2)!(l_2-m_2)!(l_3+m_3)!(l_3-m_3)!}{(l_1+l_2+l_3+1)!}} \times \sum_k \frac{(-1)^k}{k!(l_1+l_2-l_3-k)!(l_1-m_1-k)!(l_2+m_2-k)!(l_3-l_2+m_1+k)!(l_3-l_1-m_2+k)!}. \tag{B6}$$

The coefficients $g^l_{l_1m_1,l_2m_2}$ in Eq. (B4) are slightly modified versions of the Gaunt coefficients [48].

Finally, the integrals of associated Legendre functions are known for $l \geqslant m \geqslant 0$ [50],

$$A_{lm} = \int_{-1}^{1} dx P_{lm}(x) = \begin{cases} 2 & \text{if } l = m = 0 \\ \frac{2m}{l}\frac{[(l/2)!]^2(l+m)!}{[(l-m)/2]![(l+m)/2]!(l+1)!} & \text{if } l \text{ and } m \text{ are even} \\ \frac{\pi m}{2^{2l+1}l}\frac{(l+1)!(l+m)!}{([(l+1)/2]!)^2[(l-m)/2]![(l+m)/2]!} & \text{if } l \text{ and } m \text{ are odd} \\ 0 & \text{otherwise} \end{cases}.$$

The other values can be deduced from the definition of P_{lm} for negative values of l or m.

Using this last result with the multiplication formula, we can compute the integrals of product of associated Legendre functions. For example,

$$I^{l_1m_1}_{l_2,m_2} = \int_{-1}^{1} dx\, P_{l_1m_1}(x)P_{l_2m_2}(x) = \sum_{l=|l_1-l_2|}^{l_1+l_2} g^l_{l_1m_1,l_2m_2} A_{lm_1+m_2}, \tag{B7}$$

for any integral value of l_1, l_2, m_1, and m_2.

APPENDIX C: ROTATION OF PAW STRENGTH

We know that the complex spherical harmonics $Y_{lm}(\hat{r})$, under a rotation R parametrized by the Euler angles α, β, and γ, transforms according to

$$RY_{lm}(\hat{r}) = Y_{lm}(R^{-1}\hat{r}) = \sum_{m'=-l}^{l} Y_{lm'}(\hat{r})D^l_{m'm}(\alpha,\beta,\gamma), \tag{C1}$$

where $D^l_{m'm}(\alpha,\beta,\gamma)$ is the Wigner matrix [49],

$$D^l_{m'm}(\alpha,\beta,\gamma) = e^{-i\alpha m'}\langle lm'|e^{-i\beta L_y/\hbar}|lm\rangle e^{-i\gamma m}. \tag{C2}$$

For an improper rotation S, which can appear in the set of space group operations, we simply write $S = Ri$, where i is the inversion. This gives

$$SY_{lm}(\hat{r}) = \sum_{m'=-l}^{l} Y_{lm'}(\hat{r})\mathcal{D}^l_{m'm}(\alpha,\beta,\gamma) \tag{C3}$$

with $\mathcal{D}^l_{m'm}(\alpha,\beta,\gamma) = (-1)^l D^l_{m'm}(\alpha,\beta,\gamma)$.

The real spherical harmonics that we use can be related to the complex spherical harmonics as

$$S_{lm}(\hat{r}) = \sum_{m'=-l}^{l} Y_{lm'}(\hat{r}) C^{l}_{m'm}, \tag{C4}$$

where

$$C^{l}_{m'm} = \begin{cases} 1 & \text{if} \quad m = m' = 0 \\ (-1)^m/\sqrt{2} & \text{if} \quad m = m' \quad \text{and} \quad m > 0 \\ 1/\sqrt{2} & \text{if} \quad m = -m' \quad \text{and} \quad m > 0 \\ i/\sqrt{2} & \text{if} \quad m = m' \quad \text{and} \quad m < 0 \\ (-1)^m/i\sqrt{2} & \text{if} \quad m = -m' \quad \text{and} \quad m < 0 \\ 0 & \text{otherwise} \end{cases}. \tag{C5}$$

This gives

$$\Delta^{l} = C^{l+} \mathcal{D}^{l} C^{l}, \tag{C6}$$

and Δ^l is unitary because C^l and $\mathcal{D}^l$ are.

APPENDIX D: DERIVATIVES OF (PSEUDO)ORBITALS: DERIVATION

In this section, we want to compute the matrix $R_{LL'}(l\tau)$ which is defined at Eq. (73). To obtain the final formula we will need several properties of the associated Legendre functions $P_{lm}(x)$ which have been summarized in Appendix B.

To obtain $R_{LL'}(l\tau)$, we need to compute

$$\left\langle \phi_{l\tau L_1} \middle| \frac{d}{dR_{l\tau}} \phi_{l\tau L_2} \right\rangle = -\int d^3 r \, \phi^{*}_{n_1 l_1 m_1}(\mathbf{r}) \nabla \phi_{n_2 l_2 m_2}(\mathbf{r}). \tag{D1}$$

Using spherical coordinates, the gradient of an orbital can be written as

$$\begin{aligned} \nabla \phi_{nlm}(\mathbf{r}) &= \nabla R_{nl}(r) S_{lm}(\hat{\mathbf{r}}) + R_{nl}(r) \nabla S_{lm}(\hat{\mathbf{r}}) \\ &= \frac{dR_{nl}(r)}{dr} \begin{pmatrix} S_{lm}(\hat{\mathbf{r}}) \sin\theta \cos\varphi \\ S_{lm}(\hat{\mathbf{r}}) \sin\theta \sin\varphi \\ S_{lm}(\hat{\mathbf{r}}) \cos\theta \end{pmatrix} + \frac{R_{nl}(r)}{r} \begin{pmatrix} \frac{\partial S_{lm}(\hat{\mathbf{r}})}{\partial\theta} \cos\theta \cos\varphi - \frac{1}{\sin\theta} \frac{\partial S_{lm}(\hat{\mathbf{r}})}{\partial\varphi} \sin\varphi \\ \frac{\partial S_{lm}(\hat{\mathbf{r}})}{\partial\theta} \cos\theta \sin\varphi + \frac{1}{\sin\theta} \frac{\partial S_{lm}(\hat{\mathbf{r}})}{\partial\varphi} \cos\varphi \\ -\frac{\partial S_{lm}(\hat{\mathbf{r}})}{\partial\theta} \sin\theta \end{pmatrix}. \end{aligned}$$

The angular derivatives can be computed using Eq. (B2) and the recurrence relations in Appendix B. Using $x = \cos\theta$, $-1 \leqslant x \leqslant 1$, we obtain

$$\begin{aligned} \frac{\partial S_{lm}(\hat{\mathbf{r}})}{\partial\varphi} &= N_{l|m|} P_{l|m|}(x) c'_m(\varphi), \\ \frac{\partial S_{lm}(\hat{\mathbf{r}})}{\partial\theta} &= -\frac{1}{2} N_{l|m|} c_m(\varphi) [P_{l|m|+1}(x) - (l+|m|)(l-|m|+1) P_{l|m|-1}(x)]. \end{aligned}$$

To perform the integration in Eq. (D1), it is useful to rewrite this equation as a matrix product splitting the coordinates r, φ, and x.

$$\begin{aligned} \nabla \phi_{nlm}(\mathbf{r}) = {} & N_{l|m|} \frac{dR_{nl}(r)}{dr} \begin{pmatrix} c_m \cos\varphi & 0 & 0 \\ 0 & c_m \sin\varphi & 0 \\ 0 & 0 & c_m \end{pmatrix} \begin{pmatrix} \sqrt{1-x^2} P_{l|m|}(x) \\ \sqrt{1-x^2} P_{l|m|}(x) \\ x P_{l|m|}(x) \end{pmatrix} \\ & + N_{l|m|} \frac{R_{nl}(r)}{r} \begin{pmatrix} c_m \cos\varphi & 0 & 0 \\ 0 & c_m \sin\varphi & 0 \\ 0 & 0 & c_m \end{pmatrix} \begin{pmatrix} -\frac{1}{2}[x P_{l|m|+1}(x) - (l+|m|)(l-|m|+1) x P_{l|m|-1}(x)] \\ -\frac{1}{2}[x P_{l|m|+1}(x) - (l+|m|)(l-|m|+1) x P_{l|m|-1}(x)] \\ \frac{1}{2}[\sqrt{1-x^2} P_{l|m|+1}(x) - (l+|m|)(l-|m|+1)\sqrt{1-x^2} P_{l|m|-1}(x)] \end{pmatrix} \\ & + N_{l|m|} \frac{R_{nl}(r)}{r} \begin{pmatrix} c'_m \sin\varphi & 0 & 0 \\ 0 & c'_m \cos\varphi & 0 \\ 0 & 0 & 0 \end{pmatrix} \begin{pmatrix} -\frac{1}{\sqrt{1-x^2}} P_{l|m|}(x) \\ \frac{1}{\sqrt{1-x^2}} P_{l|m|}(x) \\ 0 \end{pmatrix}. \end{aligned}$$

Using again the recurrence relations for associated Legendre function in Appendix B, this can be simplified to

$$\nabla\phi_{nlm}(\mathbf{r}) = \frac{N_{l|m|}}{2l+1}\frac{dR_{nl}(r)}{dr}\mathbf{T}^0_m(\varphi)\mathbf{A}_{l|m|}\mathbf{P}_{l|m|}(x) - \frac{N_{l|m|}}{2(2l+1)}\frac{R_{nl}(r)}{r}\mathbf{T}^0_m(\varphi)\mathbf{B}_{l|m|}\mathbf{P}_{l|m|}(x) - \frac{1}{2}N_{l|m|}\frac{R_{nl}(r)}{r}\mathbf{T}^1_m(\varphi)\mathbf{C}_{l|m|}\mathbf{P}_{l|m|}(x),$$

where we have defined

$$\mathbf{T}^0_m(\varphi) = \mathrm{diag}(c_m\cos\varphi,\, c_m\sin\varphi,\, c_m),$$

$$\mathbf{T}^1_m(\varphi) = \mathrm{diag}\left(\frac{c'_m}{|m|}\sin\varphi,\, \frac{c'_m}{|m|}\cos\varphi,\, 0\right) \quad \text{if } m\neq 0, \text{ and } \mathbf{T}^1_0(\varphi) = 0,$$

$$\mathbf{A}_{l|m|} = \begin{pmatrix} 0 & 0 & -1 & 0 & 0 & 1\\ 0 & 0 & -1 & 0 & 0 & 1\\ 0 & l+|m| & 0 & 0 & l-|m|+1 & 0\end{pmatrix},$$

$$\mathbf{B}_{l|m|} = \begin{pmatrix} -(l+|m|)(l-|m|+1)(l+|m|-1) & 0 & l+|m|+1\\ -(l+|m|)(l-|m|+1)(l+|m|-1) & 0 & l+|m|+1\\ 0 & -(2l+2)(l+|m|) & 0\\ -(l+|m|)(l-|m|+1)(l-|m|+2) & 0 & l-|m|\\ -(l+|m|)(l-|m|+1)(l-|m|+2) & 0 & l-|m|\\ 0 & 2l(l-|m|+1) & 0\end{pmatrix},$$

$$\mathbf{C}_{l|m|} = \begin{pmatrix} 0 & 0 & 0 & (l-|m|+1)(l-|m|+2) & 0 & 1\\ 0 & 0 & 0 & -(l-|m|+1)(l-|m|+2) & 0 & -1\\ 0 & 0 & 0 & 0 & 0 & 0\end{pmatrix},$$

$$\mathbf{P}_{l|m|}(x) = [P_{l-1|m|-1}(x),\, P_{l-1|m|}(x),\, P_{l-1|m|+1}(x),\, P_{l+1|m|-1}(x),\, P_{l+1|m|}(x),\, P_{l+1|m|+1}(x)]^t.$$

This gives

$$\int d^3r\,\phi^*_{n_1l_1m_1}(\mathbf{r})\nabla\phi_{n_2l_2m_2}(\mathbf{r}) = \frac{N_{l_1|m_1|}N_{l_2|m_2|}}{2l_2+1}R^0_{n_1l_1,n_2l_2}\mathbf{T}^0_{m_1m_2}\mathbf{A}_{l_2|m_2|}\mathbf{P}_{l_1|m_1|,l_2|m_2|} - \frac{N_{l_1|m_1|}N_{l_2|m_2|}}{2(2l_2+1)}R^1_{n_1l_1,n_2l_2}\mathbf{T}^0_{m_1m_2}\mathbf{B}_{l_2|m_2|}\mathbf{P}_{l_1|m_1|,l_2|m_2|}$$
$$- \frac{1}{2}N_{l_1|m_1|}N_{l_2|m_2|}R^1_{n_1l_1,n_2l_2}\mathbf{T}^1_{m_1m_2}\mathbf{C}_{l_2|m_2|}\mathbf{P}_{l_1|m_1|,l_2|m_2|} \tag{D2}$$

with the radial integrals defined as

$$R^0_{n_1l_1,n_2l_2} = \int_0^{r_0} dr\, r^2 R_{n_1l_1}(r)\frac{dR_{n_2l_2}(r)}{dr}, \tag{D3}$$

$$R^1_{n_1l_1,n_2l_2} = \int_0^{r_0} dr\, r^2 R_{n_1l_1}(r)\frac{R_{n_2l_2}(r)}{r}. \tag{D4}$$

The other matrices in Eq. (D2) are integrals of the quantities defined above.

The elements of matrix $\mathbf{P}_{l_1|m_1|,l_2|m_2|}$ are integral of a product of two associated Legendre functions,

$$\mathbf{P}_{l_1|m_1|,l_2|m_2|} = \int_{-1}^{1} dx\, P_{l_1|m_1|}(x)\mathbf{P}_{l_2|m_2|}(x)$$
$$= \left[I^{l_1|m_1|}_{l_2-1|m_2|-1},\, I^{l_1|m_1|}_{l_2-1|m_2|},\, I^{l_1|m_1|}_{l_2-1|m_2|+1},\, I^{l_1|m_1|}_{l_2+1|m_2|-1},\, I^{l_1|m_1|}_{l_2+1|m_2|},\, I^{l_1|m_1|}_{l_2+1|m_2|+1}\right]^t.$$

Therefore they can be computed using Gaunt coefficients, as explained in Appendix B at Eq. (B7).

The integrals over the azimuthal angle are

$$\mathbf{T}^0_{m_1m_2} = \int_0^{2\pi} d\varphi\, c_{m_1}(\varphi)\mathbf{T}^0_{m_2}(\varphi)$$
$$= \mathrm{diag}\left(\begin{cases}\pi & \text{if } m_1m_2>0 \text{ and } |m_1-m_2|=1\\ \sqrt{2}\pi & \text{if } (m_1=0\, m_2=1) \text{ or } (m_1=1\, m_2=0)\end{cases}\right.$$
$$\left.\begin{cases}-\pi\,\mathrm{sg}(m_1+m_2) & \text{if } m_1m_2<0 \text{ and } |m_1+m_2|=1\\ \sqrt{2}\pi & \text{if } (m_1=0\, m_2=-1) \text{ or } (m_1=-1\, m_2=0)\end{cases}\right.$$
$$\left.2\pi \quad \text{if } m_1=m_2\right),$$

$$\mathbf{T}^1_{m_1m_2} = \int_0^{2\pi} d\varphi\, c_{m_1}(\varphi)\mathbf{T}^1_{m_2}(\varphi)$$
$$= \mathrm{diag}\begin{pmatrix} \begin{cases} \pi\ \mathrm{sg}(m_1)\mathrm{sg}(m_1-m_2) & \text{if } m_1m_2>0 \text{ and } |m_1-m_2|=1 \\ -\sqrt{2}\pi & \text{if } (m_1=0\, m_2=1) \end{cases} \\ \begin{cases} \pi\ \mathrm{sg}(m_1) & \text{if } m_1m_2<0 \text{ and } |m_1+m_2|=1 \\ \sqrt{2}\pi & \text{if } (m_1=0\, m_2=-1) \end{cases} \\ 0 \end{pmatrix}.$$

Collecting the above results, we obtain for $R_{L_1L_2}(l\tau)$

$$\begin{aligned} R_{L_1L_2}(l\tau) = &-\frac{N_{l_1|m_1|}N_{l_2|m_2|}}{2l_2+1}\left(R^0_{n_1l_1,n_2l_2}-\tilde{R}^0_{n_1l_1,n_2l_2}\right)\mathbf{T}^0_{m_1m_2}\mathbf{A}_{l_2|m_2|}\mathbf{P}_{l_1|m_1|,l_2|m_2|} \\ &+\frac{N_{l_1|m_1|}N_{l_2|m_2|}}{2(2l_2+1)}\left(R^1_{n_1l_1,n_2l_2}-\tilde{R}^1_{n_1l_1,n_2l_2}\right)\mathbf{T}^0_{m_1m_2}\mathbf{B}_{l_2|m_2|}\mathbf{P}_{l_1|m_1|,l_2|m_2|} \\ &+\frac{1}{2}N_{l_1|m_1|}N_{l_2|m_2|}\left(R^1_{n_1l_1,n_2l_2}-\tilde{R}^1_{n_1l_1,n_2l_2}\right)\mathbf{T}^1_{m_1m_2}\mathbf{C}_{l|_2m_2|}\mathbf{P}_{l_1|m_1|,l_2|m_2|}, \end{aligned} \tag{D5}$$

where $\tilde{R}^{0,1}_{n_1l_1,n_2l_2}$ are the radial integrals computed with the pseudo-orbiltals.

[1] A. Jain, S. P. Ong, G. Hautier, W. Chen, W. D. Richards, S. Dacek, S. Cholia, D. Gunter, D. Skinner, G. Ceder, and K. A. Persson, APL Mater. **1**, 011002 (2013).
[2] G. Pizzi, A. Cepellotti, R. Sabatini, N. Marzari, and B. Kozinsky, Comput. Mater. Sci. **111**, 218 (2016).
[3] K. Mathew, J. H. Montoya, A. Faghaninia, S. Dwarakanath, M. Aykol, H. Tang, I.-heng Chu, T. Smidt, B. Bocklund, M. Horton, J. Dagdelen, B. Wood, Z.-K. Liu, J. Neaton, S. P. Ong, K. Persson, and A. Jain, Comput. Mater. Sci. **139**, 140 (2017).
[4] A. Togo, Phonon database at kyoto university, http://phonondb.mtl.kyoto-u.ac.jp/.
[5] P. B. Allen and B. Mitrović, *Theory of Superconducting Tc*, edited by H. Ehrenreich, F. Seitz, and D. Turnbull, Solid State Physics Vol. 37 (Academic Press, 1983), pp. 1–92.
[6] H. Choi, D. Roundy, H. Sun, M. Cohen, and S. Louie, Nature (London) **418**, 758 (2002).
[7] J. M. Ziman, *Electrons and Phonons: The Theory of Transport Phenomena in Solids* (Clarendon Press, 1960).
[8] N. Medvedev, Z. Li, and B. Ziaja, Phys. Rev. B **91**, 054113 (2015).
[9] M. P. Jiang, M. Trigo, I. Savić, S. Fahy, É. D. Murray, C. Bray, J. Clark, T. Henighan, M. Kozina, M. Chollet, J. M. Glownia, M. C. Hoffmann, D. Zhu, O. Delaire, A. F. May, B. C. Sales, A. M. Lindenberg, P. Zalden, T. Sato, R. Merlin, and D. A. Reis, Nat. Commun. **7**, 12291 (2016).
[10] S. Baroni, P. Giannozzi, and A. Testa, Phys. Rev. Lett. **58**, 1861 (1987).
[11] Z. Li, G. Antonius, M. Wu, F. H. da Jornada, and S. G. Louie, Phys. Rev. Lett. **122**, 186402 (2019).
[12] W. Li, Phys. Rev. B **92**, 075405 (2015).
[13] F. Giustino, M. L. Cohen, and S. G. Louie, Phys. Rev. B **76**, 165108 (2007).
[14] J. I. Mustafa, S. Coh, M. L. Cohen, and S. G. Louie, Phys. Rev. B **92**, 165134 (2015).
[15] K. S. Thygesen, L. B. Hansen, and K. W. Jacobsen, Phys. Rev. Lett. **94**, 026405 (2005).
[16] R. Sakuma, Phys. Rev. B **87**, 235109 (2013).
[17] A. Togo and I. Tanaka, Scr. Mater. **108**, 1 (2015).
[18] L. Chaput, A. Togo, I. Tanaka, and G. Hug, Phys. Rev. B **84**, 094302 (2011).
[19] L. Chaput, Phys. Rev. Lett. **110**, 265506 (2013).
[20] A. Togo, L. Chaput, and I. Tanaka, Phys. Rev. B **91**, 094306 (2015).
[21] M. Born and K. Huang, *Dynamical Theory of Crystal Lattices* (Clarendon Press, Oxford, England, 1954).
[22] M. V. Berry, Proc. R. Soc. London A **392**, 45 (1984).
[23] R. C. Albers, L. Bohlin, M. Roy, and J. W. Wilkins, Phys. Rev. B **13**, 768 (1976).
[24] F. Giustino, Rev. Mod. Phys. **89**, 015003 (2017).
[25] F. Bloch, Z. Phys. **52**, 555 (1929).
[26] H. Fröhlich, Phys. Rev. **79**, 845 (1950).
[27] J. M. Ziman, Math. Proc. Cambridge Philos. Soc. **51**, 707 (1955).
[28] J. C. Taylor, Proc. Cambridge Phil. Soc. **52**, 693 (1956).
[29] P. E. Blöchl, Phys. Rev. B **50**, 17953 (1994).
[30] G. Kresse and D. Joubert, Phys. Rev. B **59**, 1758 (1999).
[31] G. Kresse and J. Furthmüller, Comput. Mater. Sci. **6**, 15 (1996).
[32] G. Kresse, J. Non-Cryst. Solids **192-193**, 222 (1995).
[33] S. Y. Savrasov, Phys. Rev. B **54**, 16470 (1996).
[34] S. Y. Savrasov and D. Y. Savrasov, Phys. Rev. B **54**, 16487 (1996).
[35] P. Pulay, Mol. Phys. **17**, 197 (1969).
[36] S. Goedecker and K. Maschke, Phys. Rev. B **45**, 1597 (1992).
[37] J. W. Cooley and J. W. Tukey, Math. Comput. **19**, 297 (1965).
[38] J. Keiner, S. Kunis, and D. Potts, ACM Trans. Math. Softw. **36**, 1 (2009).
[39] J. P. Perdew, K. Burke, and M. Ernzerhof, Phys. Rev. Lett. **77**, 3865 (1996).

[40] R. Bauer, A. Schmid, P. Pavone, and D. Strauch, Phys. Rev. B **57**, 11276 (1998).
[41] G. Grimvall, *The Electron-Phonon Interaction in Metals*, Selected Topics in Solid State Physics (Elsevier, North-Holland, 1981).
[42] C. B. Walker, Phys. Rev. **103**, 547 (1956).
[43] W. L. McMillan, Phys. Rev. **167**, 331 (1968).
[44] P. B. Allen and R. C. Dynes, Phys. Rev. B **12**, 905 (1975).
[45] P. B. Allen, Phys. Rev. B **17**, 3725 (1978).
[46] D. Strauch, A. P. Mayer, and B. Dorner, Z. Phys. B Condens. Matter **78**, 405 (1990).
[47] X. Blase, C. Adessi, and D. Connétable, Phys. Rev. Lett. **93**, 237004 (2004).
[48] A. R. Edmonds, *Angular Momentum in Quantum Mechanics*, 2nd ed. (Princeton University Press, Princeton, NJ, 1960).
[49] J. J. Sakurai, *Modern Quantum Mechanics* (Addison-Wesley, Reading, MA, 1994).
[50] D. W. Jepsen, E. F. Haugh, and J. O. Hirschfelder, Proc. Natl. Acad. Sci. USA **41**, 645 (1955).